Quaternary Science Reviews 312 (2023) 108173

Contents lists available at ScienceDirect

Quaternary Science Reviews

journal homepage: www.elsevier.com/locate/quascirev

# A Holocene tephrochronological framework for Finland

Maarit Kalliokoski [a, b, *], Esther Ruth Guðmundsdóttir [a], Stefan Wastegård [c], Sami Jokinen [d], Timo Saarinen [b]

[a] Nordic Volcanological Center, Institute of Earth Sciences, University of Iceland, Sturlugata 7, 102, Reykjavik, Iceland
[b] Department of Geography and Geology, University of Turku, 20014, Turun yliopisto, Finland
[c] Department of Physical Geography, Stockholm University, 10691, Stockholm, Sweden
[d] Geological Survey of Finland, Espoo, PL 96, 02151, Espoo, Finland

ARTICLE INFO

*Article history:*
Received 2 April 2023
Received in revised form
30 May 2023
Accepted 4 June 2023
Available online 15 June 2023

Handling Editor: Giovanni Zanchetta

*Keywords:*
Holocene
Fennoscandia
Geochronology
Finnish tephrochronology
Cryptotephra
Hekla Y
Aniakchak tephra
Hekla Ö
WRAe

ABSTRACT

Regional tephrochronological frameworks serve as dating and correlating tools that enable critical assessment of the validity of single cryptotephra findings. In this study, our aim was to construct an outline for a Finnish Holocene tephra framework by investigating 12 peatlands and one lake site for presence of cryptotephra. As a result, glass shards from 19 individual tephras were geochemically characterized and correlated to their source volcanoes in Iceland and Alaska. Fifteen of these tephras were identified in Finland for the first time. The oldest identified cryptotephra in the Finnish environmental records is the 7 ka Hekla 5 tephra, and the youngest one is the Askja 1875. The identification of two Alaskan tephras (White River Ash eastern lobe and Aniakchak tephra) in Finland demonstrates an opportunity for intercontinental tephra correlations. The first Finnish Holocene tephrochronology presented here reveals a great potential for using tephrochronology as a dating method in Finland and is expected to aid in future cryptotephra research in the region. Additionally, the cryptotephra findings in this study help to refine the dispersal areas of several Holocene tephras.



## 1. Introduction

Tephrochronology is an unparalleled correlating and dating tool of environmental archives in terms of temporal precision, which is manifested by the gradual expansion of the method from proximal (e.g. Thorarinsson, 1944; Björck et al., 1992) to distal (e.g. Persson, 1966; Dugmore, 1989; Pilcher and Hall, 1992; Wastegård et al., 1998; Davies, 2015) and even ultra-distal (crypto)tephra studies (e.g. Jensen et al., 2014; van der Bilt et al., 2017; Plunkett and Pilcher, 2018; Haflidason et al., 2019). The strength of tephrochronology as a geochronological tool lies in the ability of explosive volcanic eruptions to form tephra isochrons that are deposited practically instantaneously across wide regions and preserved as dating and correlation horizons in a range of environmental records (e.g. Lowe, 2011; Davies, 2015). Tephrochronology gives best results when geochemically fingerprinted tephras are stacked into well-dated regional tephra frameworks where stratigraphic and geographic relations of tephra horizons aid in evaluating the reliability of the obtained ages. The northern European distal cryptotephra frameworks consist mainly of Icelandic tephras (e.g. Wastegård, 2005; Lawson et al., 2012), but cryptotephra from other continents and volcanic centres has been identified at an increasing number of sites during the past decade (Jensen et al., 2014; Johansson et al., 2017; Plunkett and Pilcher, 2018; Jones et al., 2019; Kinder et al., 2020), offering tie-points for hemispheric correlations of environmental archives and great potential for further refining regional tephrochronologies.

Important advances have been made in tephra studies in northern Europe in the recent past both in terms of improving the Icelandic proximal tephrochronology (Óladóttir et al., 2008, 2011a, 2011b; Guðmundsdóttir et al., 2011a, 2016; Harning et al., 2018; Larsen et al., 2020) and knowledge of the dispersal areas of Holocene tephras. For example, Lawson et al. (2012) identified several regions in northern Europe where no or very few cryptotephra

* Corresponding author. Nordic Volcanological Center, Institute of Earth Sciences, University of Iceland, Sturlugata 7, 102, Reykjavik, Iceland.
*E-mail addresses:* mhk1@hi.is, mkalli@utu.fi (M. Kalliokoski).

https://doi.org/10.1016/j.quascirev.2023.108173

studies had been conducted thus far and concluded that the spatial gaps in tephra research were an important limiting factor for determining tephra dispersal patterns and fall-out frequencies. Since then, multiple studies have been published from these previously understudied areas and steps towards constructing regional tephrochronologies have been taken (e.g. Housley et al., 2013; Wulf et al., 2013, 2016; Stivrins et al., 2016; Tylmann et al., 2016; Watson et al., 2016; Jones et al., 2017, 2019; Cooper et al., 2019a; Kalliokoski et al., 2019, 2020; Kinder et al., 2020; Walsh et al., 2021). Another important aspect of improving the northern European tephra framework is establishing robust correlations between distal and proximal tephrochronologies. Even if tephra correlations between distal sites increase the value of sporadic cryptotephra findings as geochronological horizons, tracing the distal deposits to proximal tephra records is necessary for verifying their source eruptions, position in the tephrostratigraphy and the primary nature of the deposits, and here the high quality of the proximal tephrochronology is critically important.

In general, the silicic major tephra marker layers that form the foundation of the Icelandic tephrochronology have been geochemically well-characterized. However, the sheer number of active Icelandic volcanic systems that have erupted frequently during the Late Glacial and the Holocene may create difficulties when assigning distal cryptotephra deposits to their source eruptions (e.g. Larsen and Eiríksson, 2008). For example, the geochemistry and eruption histories of Snæfellsjökull, Öræfajökull and Torfajökull (and þórðarhyrna) volcanic systems are incompletely known (e.g. Haflidason et al., 2000). In the dynamic proximal area, tephra preservation potential may be low due to high erosion rates in unvegetated landscape (Larsen and Thorarinsson, 1977; Janebo et al., 2016). Additionally, older tephra layers in the vicinity of active volcanoes become inaccessible as they are buried by alternating layers of newer lava flows and thick tephra deposits. In Iceland, tephra from Snæfellsjökull, Öræfajökull and þórðarhyrna may have exceptionally low chances of preservation in terrestrial records, due to the near-shore location of these subglacial central volcanoes and repeated jökulhlaups originating from the Icelandic ice caps.

The gaps in knowledge are, however, not limited to just these volcanoes. Until recently, published data on tephra geochemistry for even some of the fairly well-known Hekla eruptions has been lacking (Larsen et al., 2020), and for example the well-known and widespread Glen Garry tephra (Dugmore and Newton, 1992; Dugmore et al., 1995; Pilcher and Hall, 1996; van den Bogaard and Schmincke, 2002; Barber et al., 2008; Watson et al., 2016; Ratcliffe et al., 2018) was correlated to a ca. 10 CE eruption of the Askja central volcano only recently (Guðmundsdóttir et al., 2016), more than two decades after its first geochemical fingerprinting in Scotland (Dugmore and Newton, 1992). A further complication in correlating the distal cryptotephra findings to their proximal counterparts are the syn-eruptive changes in geochemical composition of the volcanic products, identified for example at the Hekla central volcano (Larsen and Thorarinsson, 1977; Sverrisdóttir, 2007). The full range of geochemistry is generally present only at the proximal sites near Hekla (e.g. Jónsson et al., 2020), whereas the distal findings often represent tephra from the powerful subplinian-Plinian initial eruption phase (e.g. Larsen and Eiríksson, 2008). This combined with the effect of possible shifts in wind direction during the eruption (Guðmundsdóttir et al., 2011a; Jónsson et al., 2020) calls for a careful comparison of distal data with the proximal stratigraphy constructed from several sections representing different sectors of tephra dispersal directions.

In this study, we searched and geochemically fingerprinted glass shards from cryptotephra deposits from 13 research sites in Finland and attempted to trace each of the deposits to their source eruptions by careful comparison with proximal analytical data of tephra geochemistry along with consideration of stratigraphical and chronological constraints. In addition to geochemical analysis of tephra, we radiocarbon-dated selected tephra layers for an independent age verification of the tephrochronology. Additionally, we analysed glass from three tephra layers (Hekla X, Y and Z) from a proximal site in Iceland to establish a robust correlation for one of the cryptotephra horizons identified in Finland. As an outcome, we present here a first framework of a Holocene tephrochronology for Finland. Our results indicate a great potential for using tephrochronology as a dating method in Finland, even if difficulties do arise from using cryptotephra deposits consisting of very scarce and small shards. Finally, we publish a list of all the detected, both identified and unidentified tephra deposits with detailed descriptions and several photographs (Appendix 1) to facilitate further cryptotephra studies and application of tephrochronology in Finland and Scandinavia.

## 2. Material and methods

### 2.1. Core collection

Based on the results of a previous study on historical (younger than 870 CE) cryptotephra in Finland (Kalliokoski et al., 2020), 12 peatland sites in southern and central Finland (Fig. 1 and Table 1) were chosen for a further search of Holocene cryptotephra deposits. The research sites were selected to cover a wide geographical area of southern and central Finland, with the westernmost site located on the main island of the Åland archipelago and the easternmost site situated just 100 m west of the border zone of Finland and Russia. The full peat stratigraphy of the most promising sites in terms of the number of previously detected tephra layers was cored during the summer field seasons 2014, 2015 and 2018 using a Russian peat corer with a 50-cm-long and 5-cm-wide cylinder. The cores were taken with a 10-cm overlap from two coring points within 1 m distance from each other to ensure that the full peat depth without any gaps would be retrieved. Additionally, one lake site (Sirrajärvi, 13 in Fig. 1 and Table 1) in Northern Finland, a region where cryptotephra research had thus far not been conducted, was selected for an initial investigation. A 2-m-long lake sediment core was collected from water depth of 11.4 m in the deepest basin of Sirrajärvi with a rod-operated piston corer during the spring 2015 when ice-cover could be used as a coring platform.

Proximal samples of the two-coloured Hekla X, Y and Z tephra layers (Larsen et al., 2020) were collected in 2018 from a soil section on a riverbank (N°64.0335 W°19.3558) ca. 15 km away from the summit of the Hekla volcano. These samples were intended for electron microprobe analysis (EMPA) with the aim of improving the proximal dataset of geochemical composition of Hekla tephras, since at the time of sampling, no published geochemical data on glass from these tephra layers were available. The dark and light parts of each layer were subsampled separately throughout the thickness of the layer and the material was stored in plastic bags in cool conditions until laboratory processing.

### 2.2. Laboratory work

#### 2.2.1. Proximal samples of Hekla X, Y and Z tephras

The proximal samples of the Hekla X, Y and Z tephras were sieved through a setup of sieves with standard mesh sizes of 500, 250, 125 and 63 μm. Initially, the fraction retained on the 63 μm sieve was selected for EMPA, because it represents grain sizes that are most likely to be distally dispersed yet large enough for successful analysis. Later, also the 125–250 μm size fraction was prepared for EMPA to examine whether its geochemical composition is

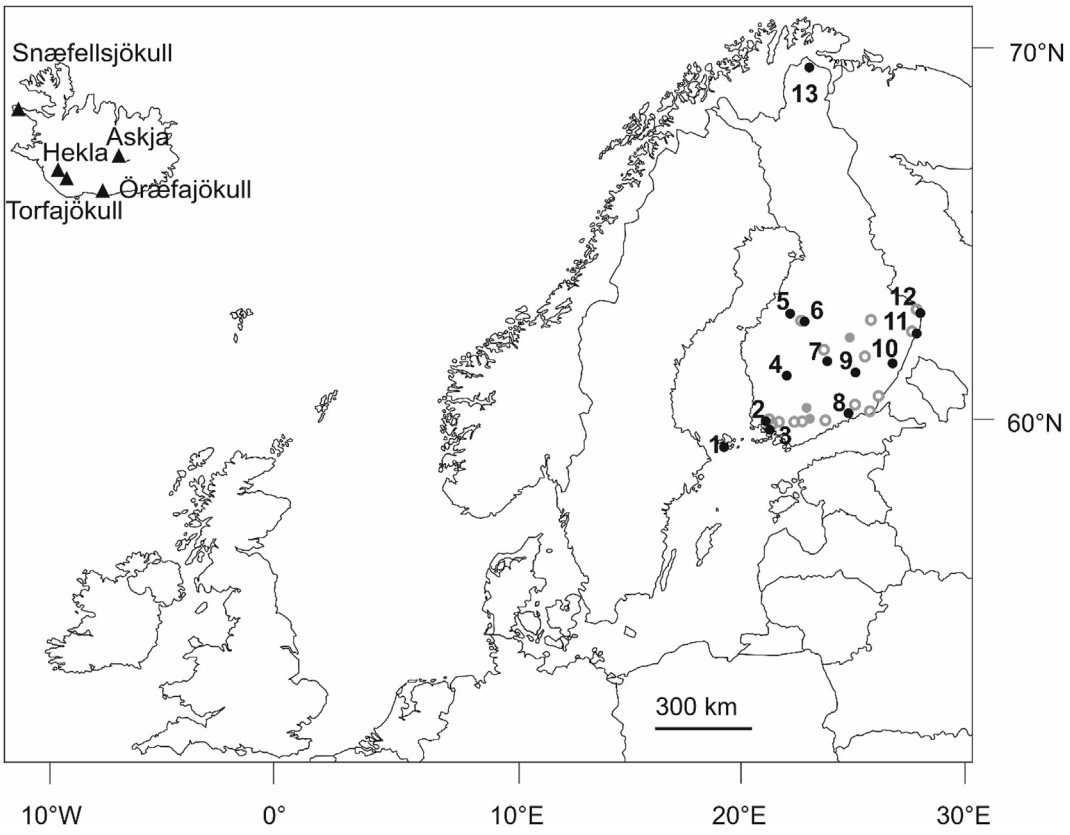


**Fig. 1.** Locations of our research sites and selected Icelandic central volcanoes. 1 = Stormossen; 2 = Kolkansuo; 3 = Rehtsuo; 4 = Suovanalanen; 5 = Kivihypönneva; 6 = Pervarvikonneva; 7 = Haapasuo; 8 = Kananiemensuo; 9 = Tarilampi; 10 = Punkaharju; 11 = Parkusuo; 12 = Hanhisuo; 13 = Sirrajärvi. Additionally, sites where cryptotephra has been previously identified are shown with grey dots. Grey circles denote sites where cryptotephra has not been detected in earlier investigations of the uppermost 50–90 cm of surface peat.

**Table 1**
Co-ordinates of the Finnish research sites. Previously reported tephras from Kalliokoski et al. (2019, 2020).

| No. | Research site (code) | Core length (cm) | Previously detected tephras | Lat. (N) | Long. (E) |
|---|---|---|---|---|---|
| 1 | Stormossen (STOR) | 90 | Two unidentified deposits | 60.12 | 19.75 |
| 2 | Kolkansuo (KOL) | 500 | – | 60.82 | 22.11 |
| 3 | Rehtsuo (REHT) | 455 | Askja 1875, Hekla 1510? | 60.60 | 22.25 |
| 4 | Suovanalanen (SUO) | 569 | Two unidentified deposits | 61.92 | 23.50 |
| 5 | Kivihypönneva (KIVI) | 247 | Unidentified, Askja 1875, Hekla 1510, Hekla 1158 | 63.50 | 24.12 |
| 6 | Pervarvikonneva (PER) | 275 | Unidentified, Hekla 1510, Hekla 1158 | 63.26 | 24.87 |
| 7 | Haapasuo (HAA) | 319 | Askja 1875 | 61.91 | 26.05 |
| 8 | Kananiemensuo (KANA) | 545 | Askja 1875, Hekla 1845, Hekla 1510 | 60.57 | 26.71 |
| 9 | Tarilampi (TAR) | 238 | Askja 1875 | 61.74 | 27.22 |
| 10 | Punkaharju (PUN) | 660 | – | 61.79 | 29.31 |
| 11 | Parkusuo (PAR) | 415 | – | 62.42 | 30.99 |
| 12 | Hanhisuo (HAN) | 312 | Askja 1875 | 62.89 | 31.51 |
| 13 | Sirrajärvi (SIR) | 206 | – | 68.53 | 22.24 |

comparable with the 63–125 μm fraction. The sieved samples contained very scarce organic matter that was removed with tweezers under a stereo microscope. Then, the samples were mounted in epoxy stubs, polished and carbon coated at the thin section laboratory of the Institute of Earth Sciences (IES), University of Iceland (UI).

### 2.2.2. Cryptotephra samples from Finnish sites

Contiguous 5–10-cm-long subsamples were initially taken from the 50-cm long peat cores and investigated for presence of cryptotephra. First, the subsamples were ashed at 550 °C for 4 h and treated with 10% HCl for 5 h for removing organic matter and carbonates. All the lake sediment samples and the peat samples that contained a substantial amount of diatoms or minerogenic matter were then sieved using 80 μm and either 10 or 25 μm meshes and subjected to heavy liquid separation (Turney, 1998). Heavy liquid densities of 2.3 and 2.6 g/cm$^3$ were used for concentrating the volcanic glass and the samples were subsequently mounted on microscope slides using Canada Balsam. Volcanic glass was identified under a polarizing microscope. The longest axis of the shards was measured, and the shards were described and photographed for compiling a catalogue of cryptotephra deposits in Finland (Appendix 1). Where glass shards were detected, 1-cm high-resolution subsamples of 2–4 cm$^3$ volume were prepared for shard counts to define the depth of peak shard concentration. If initial investigation of the 5–10-cm-long subsamples revealed a cryptotephra deposit consisting of extremely scarce shards (≤5/sample), high-resolution subsamples for shard counts were not

taken to ensure that there would be enough glass shards left in the core material for EMPA.

Fresh samples for geochemical fingerprinting of tephra were taken from the depth of peak shard concentration or from the 5-cm intervals of peat where scarce volcanic glass had been detected. The samples for EMPA were treated with acid digestion method instead of ashing to avoid alteration of volcanic glass during combustion (Pilcher and Hall, 1992; Dugmore et al., 1995). Where necessary, samples were sieved and then cleaned by heavy liquid floatation (with sodium polytungstate of 2.3 g/cm$^3$ density). If the samples contained very scarce glass shards in a dense matrix of biogenic silica and minerogenic matter, the shards were hand-picked using a micromanipulator with an attached gas chromatography syringe and a needle (Lane et al., 2014; MacLeod et al., 2014). All the samples for EMPA were mounted on glass slides with epoxy, sanded and polished down to a thickness of 8–25 μm and carbon-coated. At Haapasuo site, 2-cm-thick samples from the depth of 130–140 cm were presumed to contain basaltic glass based on the brown colour of the shards under microscope and thus were prepared for EMPA differently from the other samples in this study. The fresh peat was first wet sieved through 80 and 10 μm meshes and the fraction remaining on the 10 μm mesh was cleaned from organic matter using heavy liquid of 2.3 g/cm$^3$ density. To avoid potential alteration of basaltic glass during acid digestion process (Blockley et al., 2005; Cooper et al., 2019b), the >2.3 g/cm$^3$ fraction was next treated with hot, concentrated acids just for <10 min, in which time all the remaining organic matter had dissolved and the residue consisted of clean glass shards and minor amount of minerogenic grains.

### 2.3. Electron microprobe analysis

Geochemical composition of the proximal samples of Hekla X, Y and Z tephras was determined by analysing at least 20 volcanic glass grains along randomly selected lines in the epoxy stubs (Guðmundsdóttir et al., 2011b). For geochemical characterization of the cryptotephra deposits from the Finnish sites, point analysis was conducted on every shard exposed on the sample surface. In some samples a second round of sanding and polishing was necessary after analysing the largest shards, so that the smallest shards could also be brought to the sample surface and analysed. Analysis of ten major elements was performed using wavelength dispersive spectrometry either on the JEOL JXA-8230 SuperProbe at the IES, UI or the Cameca SX100 microprobe at the Tephra Analysis Unit (TAU) of the University of Edinburgh. More information on the microprobe configurations and performing the analysis is available in Supplementary Table S1. Two samples (Parkusuo 95 and Pervarvikonneva 115) were analysed at both facilities to verify that the microprobes at the TAU and the IES produce comparable results with the settings used in this study, since the microprobe at the IES had been used only once before for cryptotephra analysis (Kalliokoski et al., 2020).

### 2.4. Radiocarbon dating

Samples for radiocarbon dating the cryptotephra deposits were collected from Kivihypönneva (site 5 in Fig. 1) peat core that contains the highest number of tephra layers (Figs. 2 and 3). Additionally, one sample was taken from Parkusuo, from the depth of a prominent cryptotephra layer. Moss (Sphagnum sp.) stems and leaves were picked from the depth of the peak glass shard concentration if there was core material left. Otherwise, the $^{14}$C samples were collected immediately above or below the peak for constraining the minimum or maximum age for the tephra in question. The samples were radiocarbon dated at the Aarhus AMS Centre and the obtained radiocarbon ages were calibrated using the

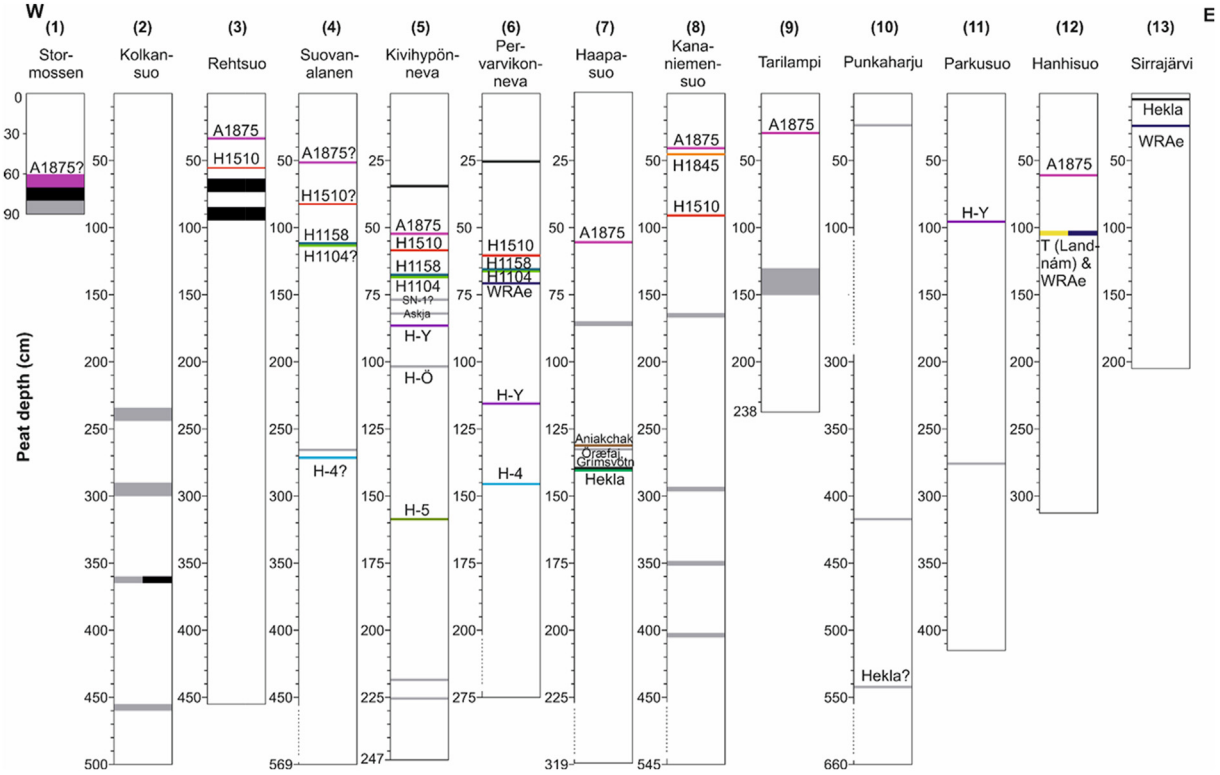


**Fig. 2.** Tephra stratigraphy of the research sites. Unidentified rhyolitic deposits are marked with grey. Deposits consisting of brownish shards are marked with black. The line thickness denotes the depth range where shards were encountered.

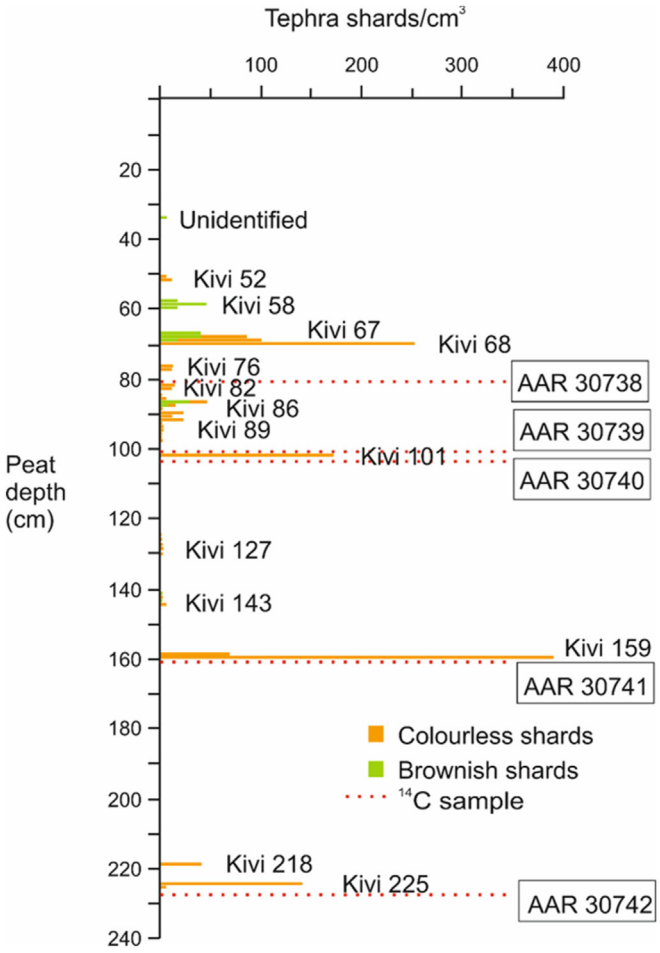


**Fig. 3.** An example of cryptotephra shard counts and locations of subsamples taken for EMPA and radiocarbon-dating from Kivihypönneva peat core.

IntCal-20 calibration curve (Reimer et al., 2020) and OxCal 4.4 online program (Bronk Ramsey, 2009). An age depth model for Kivihypönneva site was constructed with the recently developed software Undatable (Lougheed and Obrochta, 2019) that uses Bayesian radiocarbon calibration routine. Both the radiocarbon ages and the identified historical tephras (Askja, 1875; Hekla 1510, Hekla 1158, and Hekla 1104) were included in the model. As suggested by Lougheed and Obrochta (2019), we selected 0.1 for xfactor value, which determines the sediment accumulation rate uncertainty between age-depth constraints. Due to a low number of radiocarbon dates available, we refrained from using the bootstrapping function that randomly removes a selected percentage of the age-depth constraints in each run (Lougheed and Obrochta, 2019).

## 3. Results

### 3.1. Proximal samples

The EMPA of glass shards from the proximal Hekla X, Y and Z tephras in this study reveal slight differences in their geochemical compositions (Table S1). A more extensive database on the geochemistry of these and other Holocene Icelandic tephra layers was recently published by Meara et al. (2020) who report no significant differences in the geochemical composition of the Hekla "alphabet" tephras (H-A, H–B, H–C, H-M, H–N, H-X, H–Y and H-Z). In contrast, the results of XRF-analysis of tephra bulk geochemistry by Larsen et al. (2020) reveal more variability in the major element geochemistry of these layers. For example, the $SiO_2$ content of Hekla Y is higher (55.51–64.22 % wt) than that of the Hekla X (57.2–62.58%) or Hekla Z (52.71–62.95 % wt). Our results are similar to the findings of Larsen et al. (2020) with $SiO_2$ content of Hekla Y ranging between 53.17 and 65.93 % wt, slightly higher than the values for Hekla X (54.07–63.98 % wt) and Hekla Z (52.83–63.89 % wt) (Table S1). To rule out the possibility that the detected differences in the geochemical signature of the Hekla X, Y and Z tephra samples in this study would be an artefact of our sampling strategy of using a finer fraction than is common at proximal locations, a new set of samples from the same section was sieved and this time both the 63–125 μm and 125–250 μm fractions were analysed. The repeated analysis gave similar results as the first one showing slight differences between the composition of the individual Hekla X, Y and Z tephras, whereas no differences were detected between the geochemical composition of the two size fractions within the same layer (Table S1). Caution is, however, needed when establishing correlations between distal cryptotephra findings and the proximal Hekla alphabet tephras. The overlap between Hekla alphabet tephra populations is considerable, and distinctive points at the higher and lower ends of the geochemical range may be missed when the total number of analyses is small.

### 3.2. Finnish sites

The 13 research sites in this study contain 61 stratigraphically separate cryptotephra deposits, of which 37 were geochemically characterized (Fig. 2). EMPA of the scarcest deposits consisting of very small shards with thin and platy or highly vesicular morphology often failed even after repeated attempts to prepare the samples. A list of all the detected tephra deposits with their occurrence depths, description of grain morphology and shard photographs can be found in Appendix 1. This list is intended for use as a manual for further tephrochronological studies in Finland and Scandinavia. All the collected data on both the geochemically identified and unidentified tephra layers with several shard photographs are included in the list to facilitate the use of tephrochronology in the region also by researchers without previous experience in cryptotephra studies. The EMPA results of 13 cryptotephra deposits have been published earlier (Kalliokoski et al., 2019, 2020), and the full dataset of unnormalized results of the major element analysis is given for the remaining 24 layers in Supplementary Table S1 and normalised average values for the main cryptotephra deposit are listed in Table 2.

#### 3.2.1. Stormossen (1)

The peat stratigraphy of Stormossen is just 90 cm thick at our coring site. Despite multiple coring attempts, core recovery was poor due to the undecomposed nature of the peat even in the basal part of the stratigraphy. Cryptotephra was found in three consequent 10-cm-long samples. Colourless, large volcanic glass shards were detected at the 60–70 cm depth, whereas the 70–80 cm depth contains brownish shards (Fig. 1A and B in Appendix 1). At the 80–90 cm depth both colourless and brownish shards are present (Fig. 1C in Appendix 1). No shard counts or EMPA were attempted on these deposits due to poor core recovery and the assumed young age of the peat as well as disturbed stratigraphy during coring.

#### 3.2.2. Kolkansuo (2)

A 500-cm-long peat core from Kolkansuo was investigated for presence of cryptotephra. Four separate deposits were detected at

**Table 2**
Average major element compositions and standard deviations (SD) of selected cryptotephra deposits at Finnish sites. All values are normalised except for the original analytical totals. Total iron is expressed as FeO.

| Site/Sample code | | $SiO_2$ | $TiO_2$ | $Al_2O_3$ | FeO | MnO | MgO | CaO | $Na_2O$ | $K_2O$ | $P_2O_5$ | Total |
|---|---|---|---|---|---|---|---|---|---|---|---|---|
| Suovanalanen | | | | | | | | | | | | |
| SUO 112 | | | | | | | | | | | | |
| Hekla 1158 (6) | Mean | 68.27 | 0.47 | 14.99 | 5.52 | 0.20 | 0.44 | 3.06 | 4.63 | 2.33 | 0.09 | 99.09 |
| IES | SD | 0.27 | 0.03 | 0.18 | 0.16 | 0.03 | 0.02 | 0.06 | 0.20 | 0.04 | 0.04 | 0.28 |
| SUO 270 | | | | | | | | | | | | |
| Hekla 4? (1) | | 76.44 | 0.16 | 12.82 | 1.86 | 0.09 | 0.05 | 1.19 | 4.44 | 2.93 | 0.02 | 97.06 |
| Kivihypönneva | | | | | | | | | | | | |
| KIVI 52 | | | | | | | | | | | | |
| Askja 1875 (10) | Mean | 73.21 | 0.84 | 12.79 | 3.53 | 0.12 | 0.72 | 2.51 | 3.74 | 2.38 | 0.15 | 99.01 |
| IES | SD | 1.04 | 0.07 | 0.23 | 0.31 | 0.03 | 0.07 | 0.23 | 0.55 | 0.07 | 0.03 | 1.01 |
| KIVI 58 | | | | | | | | | | | | |
| Hekla 1510 (7) | Mean | 63.03 | 0.93 | 15.65 | 7.86 | 0.23 | 1.29 | 4.48 | 4.49 | 1.74 | 0.32 | 97.93 |
| IES | SD | 0.35 | 0.04 | 0.18 | 0.20 | 0.03 | 0.08 | 0.13 | 0.16 | 0.08 | 0.05 | 1.15 |
| KIVI 67 | | | | | | | | | | | | |
| Hekla 1158 (10) | Mean | 68.10 | 0.49 | 14.92 | 5.61 | 0.18 | 0.45 | 3.06 | 4.77 | 2.33 | 0.10 | 98.70 |
| IES | SD | 0.44 | 0.03 | 0.27 | 0.19 | 0.02 | 0.04 | 0.15 | 0.41 | 0.09 | 0.02 | 1.92 |
| KIVI 68 | | | | | | | | | | | | |
| Hekla 1104 (3) | Mean | 72.98 | 0.23 | 14.61 | 3.09 | 0.12 | 0.11 | 1.96 | 4.28 | 2.61 | 0.02 | 97.90 |
| IES | SD | 0.40 | 0.02 | 0.25 | 0.11 | 0.01 | 0.01 | 0.02 | 0.47 | 0.10 | 0.02 | 4.32 |
| KIVI 76 | | | | | | | | | | | | |
| SN-1 (1) | | 67.11 | 0.44 | 15.87 | 4.46 | 0.19 | 0.35 | 2.05 | 5.47 | 4.00 | 0.07 | 99.16 |
| IES | | | | | | | | | | | | |
| KIVI 82 | | | | | | | | | | | | |
| Askja (10) | Mean | 73.66 | 0.82 | 13.09 | 3.50 | 0.10 | 0.67 | 2.53 | 3.08 | 2.39 | 0.16 | 99.26 |
| IES | SD | 1.09 | 0.05 | 0.26 | 0.30 | 0.02 | 0.11 | 0.26 | 0.64 | 0.05 | 0.04 | 1.75 |
| KIVI 86 | | | | | | | | | | | | |
| Hekla Y (12) | Mean | 63.73 | 0.98 | 15.86 | 6.89 | 0.18 | 1.51 | 4.74 | 4.23 | 1.55 | 0.34 | 98.83 |
| IES | SD | 0.46 | 0.04 | 0.16 | 0.26 | 0.02 | 0.09 | 0.14 | 0.18 | 0.04 | 0.05 | 0.41 |
| KIVI 101 | | | | | | | | | | | | |
| A Hekla Ö (4) | Mean | 75.35 | 0.21 | 13.21 | 2.47 | 0.09 | 0.07 | 1.42 | 4.34 | 2.80 | 0.04 | 97.11 |
| IES | SD | 1.01 | 0.03 | 0.57 | 0.19 | 0.03 | 0.01 | 0.19 | 0.15 | 0.08 | 0.02 | 0.64 |
| B Hekla Ö (8) | Mean | 78.23 | 0.15 | 11.96 | 1.64 | 0.08 | 0.03 | 0.82 | 3.84 | 3.24 | 0.02 | 96.94 |
| IES | SD | 0.61 | 0.05 | 0.35 | 0.22 | 0.03 | 0.01 | 0.13 | 0.21 | 0.17 | 0.02 | 0.43 |
| KIVI 159 | | | | | | | | | | | | |
| Hekla 5 (12) | Mean | 76.53 | 0.11 | 13.12 | 1.67 | 0.08 | 0.04 | 1.32 | 4.43 | 2.69 | 0.02 | 97.22 |
| IES | SD | 0.42 | 0.03 | 0.34 | 0.08 | 0.03 | 0.01 | 0.14 | 0.24 | 0.13 | 0.02 | 1.08 |
| Pervarvikonneva | | | | | | | | | | | | |
| PER 60 | | | | | | | | | | | | |
| Hekla 1510 (19) | Mean | 63.05 | 0.94 | 15.63 | 7.68 | 0.22 | 1.36 | 4.58 | 4.53 | 1.70 | 0.31 | 97.83 |
| IES | SD | 0.52 | 0.04 | 0.17 | 0.35 | 0.04 | 0.09 | 0.16 | 0.31 | 0.10 | 0.04 | 1.31 |
| PER 65 | | | | | | | | | | | | |
| Hekla 1158 (5) | Mean | 68.44 | 0.47 | 14.92 | 5.61 | 0.18 | 0.45 | 3.06 | 4.44 | 2.34 | 0.09 | 98.56 |
| IES | SD | 0.13 | 0.01 | 0.22 | 0.24 | 0.01 | 0.01 | 0.08 | 0.32 | 0.05 | 0.03 | 0.60 |
| PER 66 | | | | | | | | | | | | |
| Hekla 1104 (2) | Mean | 72.90 | 0.20 | 14.44 | 3.17 | 0.10 | 0.10 | 1.97 | 4.38 | 2.70 | 0.04 | 98.66 |
| PER 69 | | | | | | | | | | | | |
| WRAe (4) | Mean | 73.97 | 0.25 | 14.58 | 1.51 | 0.05 | 0.41 | 1.94 | 4.01 | 3.21 | 0.07 | 97.14 |
| IES | SD | 0.34 | 0.04 | 0.24 | 0.06 | 0.03 | 0.05 | 0.07 | 0.22 | 0.04 | 0.04 | 1.18 |
| PER 115 | | | | | | | | | | | | |
| Hekla Y (15) | Mean | 63.92 | 0.96 | 15.86 | 6.87 | 0.18 | 1.48 | 4.77 | 4.06 | 1.53 | 0.36 | 98.42 |
| IES | SD | 0.60 | 0.06 | 0.18 | 0.35 | 0.02 | 0.09 | 0.19 | 0.41 | 0.04 | 0.04 | 1.18 |
| Hekla Y (9) | Mean | 63.08 | 0.94 | 15.96 | 7.16 | 0.18 | 1.46 | 4.74 | 4.57 | 1.64 | 0.27 | 99.59 |
| TAU | SD | 0.79 | 0.04 | 0.30 | 0.60 | 0.01 | 0.13 | 0.19 | 0.26 | 0.12 | 0.03 | 0.83 |
| PER 145 | | | | | | | | | | | | |
| Hekla 4 (5) | Mean | 76.50 | 0.09 | 12.79 | 1.95 | 0.08 | 0.03 | 1.37 | 4.17 | 3.02 | 0.01 | 96.78 |
| TAU | SD | 0.44 | 0.01 | 0.39 | 0.09 | 0.01 | 0.02 | 0.06 | 0.74 | 0.14 | 0.00 | 0.90 |
| Haapasuo | | | | | | | | | | | | |
| HAA 55 | | | | | | | | | | | | |
| Askja 1875 (9) | Mean | 73.21 | 0.81 | 12.54 | 3.53 | 0.10 | 0.69 | 2.47 | 4.11 | 2.42 | 0.11 | 99.99 |
| TAU | SD | 0.54 | 0.02 | 0.38 | 0.29 | 0.01 | 0.06 | 0.10 | 0.24 | 0.11 | 0.01 | 0.91 |
| HAA 130 | | | | | | | | | | | | |
| Grímsvötn (5) | Mean | 50.25 | 2.67 | 13.67 | 13.66 | 0.22 | 5.83 | 10.50 | 2.52 | 0.41 | 0.28 | 98.92 |
| IES | SD | 0.67 | 0.34 | 0.22 | 0.58 | 0.04 | 0.25 | 0.36 | 0.68 | 0.09 | 0.04 | 0.58 |
| HAA 132 | | | | | | | | | | | | |
| Grímsvötn (3) | Mean | 50.49 | 2.38 | 13.91 | 13.19 | 0.23 | 6.04 | 10.55 | 2.59 | 0.36 | 0.25 | 98.73 |
| IES | SD | 0.24 | 0.08 | 0.06 | 0.36 | 0.02 | 0.14 | 0.16 | 0.41 | 0.00 | 0.04 | 0.31 |
| Aniakchak (10) | Mean | 71.40 | 0.48 | 15.15 | 2.28 | 0.15 | 0.50 | 1.75 | 5.17 | 3.04 | 0.09 | 98.42 |
| IES | SD | 0.53 | 0.01 | 0.25 | 0.05 | 0.03 | 0.03 | 0.07 | 0.98 | 0.25 | 0.04 | 2.19 |
| HAA 134 | | | | | | | | | | | | |
| Grímsvötn (3) | Mean | 50.49 | 2.80 | 13.55 | 13.65 | 0.22 | 5.51 | 10.10 | 2.95 | 0.44 | 0.29 | 98.13 |
| IES | SD | 0.22 | 0.41 | 0.39 | 0.56 | 0.02 | 0.61 | 0.77 | 0.46 | 0.09 | 0.08 | 0.97 |
| Öræfajökull (11) | Mean | 73.13 | 0.24 | 13.48 | 3.22 | 0.11 | 0.01 | 0.96 | 5.14 | 3.70 | 0.01 | 97.56 |
| IES | SD | 0.36 | 0.03 | 0.20 | 0.16 | 0.02 | 0.01 | 0.07 | 0.35 | 0.21 | 0.02 | 1.64 |

**Table 2** (*continued*)

| Site/Sample code | | $SiO_2$ | $TiO_2$ | $Al_2O_3$ | FeO | MnO | MgO | CaO | $Na_2O$ | $K_2O$ | $P_2O_5$ | Total |
|---|---|---|---|---|---|---|---|---|---|---|---|---|
| HAA 136 | | | | | | | | | | | | |
| Veiðivötn (5) | Mean | 50.35 | 1.64 | 14.10 | 11.93 | 0.21 | 7.08 | 12.04 | 2.29 | 0.19 | 0.16 | 98.41 |
| IES | SD | 0.40 | 0.21 | 0.11 | 0.52 | 0.03 | 0.13 | 0.21 | 0.15 | 0.04 | 0.06 | 0.73 |
| Grímsvötn (3) | Mean | 50.40 | 2.58 | 13.54 | 13.26 | 0.22 | 5.91 | 10.73 | 2.74 | 0.39 | 0.24 | 98.52 |
| IES | SD | 1.00 | 0.37 | 0.28 | 0.61 | 0.00 | 0.78 | 1.03 | 0.34 | 0.12 | 0.06 | 0.86 |
| HAA 138 | | | | | | | | | | | | |
| Hekla (15) | Mean | 66.77 | 0.52 | 15.43 | 6.15 | 0.19 | 0.65 | 3.57 | 4.63 | 1.95 | 0.15 | 99.30 |
| IES | SD | 0.51 | 0.05 | 0.15 | 0.33 | 0.02 | 0.06 | 0.16 | 0.13 | 0.05 | 0.03 | 0.70 |
| Hekla (2) | Mean | 73.43 | 0.18 | 14.38 | 2.91 | 0.08 | 0.15 | 1.89 | 4.45 | 2.53 | 0.02 | 98.72 |
| Kverkfjöll (5) | Mean | 50.94 | 3.45 | 13.24 | 14.31 | 0.24 | 4.73 | 9.02 | 3.00 | 0.66 | 0.39 | 98.02 |
| IES | SD | 0.14 | 0.08 | 0.09 | 0.10 | 0.03 | 0.12 | 0.12 | 0.13 | 0.07 | 0.05 | 0.61 |
| Grímsvötn (7) | Mean | 50.42 | 2.47 | 13.55 | 13.71 | 0.24 | 5.64 | 10.38 | 2.93 | 0.39 | 0.27 | 98.34 |
| IES | SD | 0.55 | 0.17 | 0.18 | 0.67 | 0.03 | 0.45 | 0.55 | 0.14 | 0.11 | 0.07 | 0.58 |
| Punkaharju | | | | | | | | | | | | |
| PUN 542 | | | | | | | | | | | | |
| Hekla (2) | Mean | 72.82 | 0.23 | 14.22 | 3.07 | 0.13 | 0.09 | 1.90 | 4.65 | 2.84 | 0.06 | 98.54 |
| Parkusuo | | | | | | | | | | | | |
| PAR 95 | | | | | | | | | | | | |
| Hekla Y (20) | Mean | 63.69 | 0.95 | 15.86 | 6.83 | 0.17 | 1.42 | 4.69 | 4.57 | 1.56 | 0.27 | 99.83 |
| TAU | SD | 0.99 | 0.06 | 0.64 | 0.38 | 0.02 | 0.23 | 0.28 | 0.20 | 0.12 | 0.02 | 1.04 |
| Hekla Y (5) | Mean | 63.23 | 1.01 | 15.88 | 6.92 | 0.21 | 1.55 | 4.91 | 4.34 | 1.52 | 0.42 | 99.05 |
| IES | SD | 0.15 | 0.05 | 0.20 | 0.16 | 0.01 | 0.06 | 0.14 | 0.21 | 0.07 | 0.05 | 0.32 |
| Hanhisuo | | | | | | | | | | | | |
| HAN 60 | | | | | | | | | | | | |
| Askja 1875 (6) | Mean | 73.26 | 0.79 | 12.56 | 3.42 | 0.10 | 0.65 | 2.46 | 4.14 | 2.51 | 0.12 | 98.58 |
| TAU | SD | 0.87 | 0.03 | 0.55 | 0.18 | 0.00 | 0.04 | 0.17 | 0.20 | 0.10 | 0.01 | 1.52 |
| HAN 100 | | | | | | | | | | | | |
| A WRAe (3) | Mean | 75.61 | 0.18 | 14.07 | 1.24 | 0.05 | 0.27 | 1.64 | 3.51 | 3.41 | 0.02 | 96.31 |
| B Torfajökull (2) | Mean | 71.90 | 0.24 | 14.87 | 2.18 | 0.05 | 0.24 | 0.91 | 4.98 | 4.60 | 0.03 | 98.52 |
| Sirrajärvi | | | | | | | | | | | | |
| SIR 5 | | | | | | | | | | | | |
| Hekla (11) | Mean | 61.94 | 1.02 | 15.60 | 8.54 | 0.24 | 1.34 | 4.80 | 4.47 | 1.71 | 0.34 | 98.76 |
| IES | SD | 0.31 | 0.02 | 0.22 | 0.14 | 0.04 | 0.04 | 0.18 | 0.19 | 0.06 | 0.04 | 0.51 |
| SIR 26 | | | | | | | | | | | | |
| WRAe (3) | Mean | 74.33 | 0.26 | 14.62 | 1.53 | 0.05 | 0.39 | 1.98 | 3.73 | 3.06 | 0.05 | 96.73 |
| IES | SD | 0.29 | 0.01 | 0.11 | 0.03 | 0.03 | 0.03 | 0.07 | 0.26 | 0.01 | 0.01 | 1.60 |

the depths of 235–245 cm (platy, large, colourless), 290–300 cm (small, colourless, mostly elongated), 360–365 cm (colourless, varying morphology) and 455–460 cm (colourless, platy) (Fig. 2A–D in Appendix 1). Unfortunately, material for EMPA was lost during sample preparation due to a corroded 25 μm mesh and no geochemical results could be obtained for these deposits.

### 3.2.3. Rehtsuo (3)

Cryptotephra investigation of a 455-cm-long peat core from Rehtsuo resulted in detection of four separate tephra deposits, at 32–33 cm (large colourless), 55–56 cm (small, brownish), 65–75 cm (small, light brownish) and at 85–95 cm (small, yellowish) depths (Fig. 3A–C in Appendix 1). Of these, the two uppermost layers (Askja, 1875 and Hekla 1510) have been geochemically characterized already earlier (Kalliokoski et al., 2019, 2020). Unfortunately, the geochemical fingerprinting of the two lowermost layers failed due to a low initial number of shards and their small size that resulted in low totals in EMPA.

### 3.2.4. Suovanalanen (4)

The full core length (569 cm) from Suovanalanen was investigated for presence of cryptotephra, and six stratigraphically separate tephra deposits were identified at 51–52 cm, 82–83 cm, 112–113 cm, 114–115 cm, 266–267 cm, and 270–271 cm depths, respectively (Fig. 4A–F in Appendix 1 and Fig. 2). EMPA was successful on just two of the deposits, a dacitic Hekla tephra (SUO 112) at 112–113 cm and a rhyolitic Hekla tephra (SUO 270) at 270–271 cm depth, and only one analysis was obtained from the SUO 270 sample (Tables 2 and S1). The geochemical composition of the cryptotephra deposit at the 51–52 cm depth could not be analysed due to lack of core material for EMPA. The deposits at

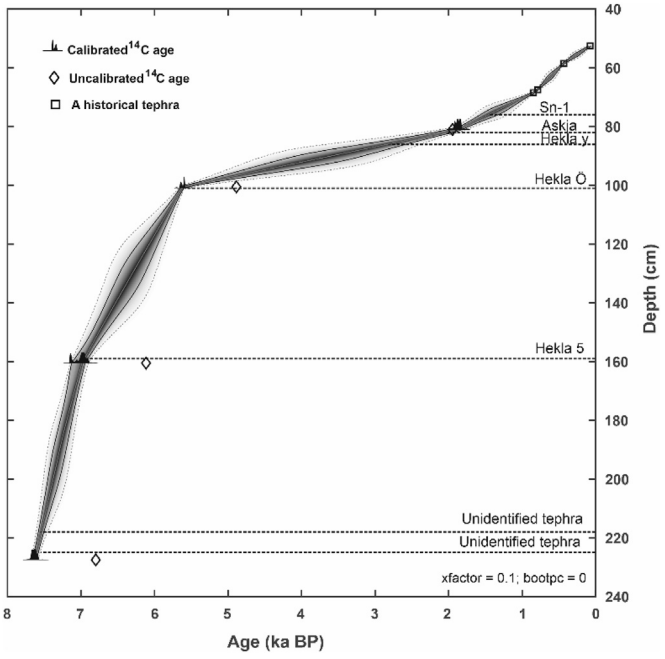


**Fig. 4.** Age depth model for Kivihypönneva site generated with Undatable (Lougheed and Obrochta, 2019). The historical tephra ages that were included in the model are indicated with squares. The 68.2% and 95.4% confidence intervals are shown as dark and lighter grey probability envelopes, respectively.

114–115 cm, and 266–267 cm depths consisted of very small and thin shards that were polished away during the final steps of the

EMPA sample preparation.

### 3.2.5. Kivihypönneva (5)

The 247-cm-thick peat stratigraphy of Kivihypönneva comprises the highest number of cryptotephra deposits in this study. Altogether, at least 13 cryptotephra deposits were detected (Fig. 5A–L in Appendix 1 and Fig. 2) at 34–35 cm, 52–53 cm, 58–59 cm, 67–68 cm, 68–69 cm, 76–78 cm, 82–83 cm, 86–87 cm, 89–90 cm, 101–102 cm, 159–160 cm, 218–219 cm and 225–226 cm depths. Additionally, two intervals with a trace amount of volcanic glass were detected at 125–130 cm and 141–144 cm depths, but EMPA on these deposits failed (Fig. 3). From this core, 12 cryptotephra horizons were geochemically characterized (Tables 2 and S1). However, very low number of successful analysis was obtained

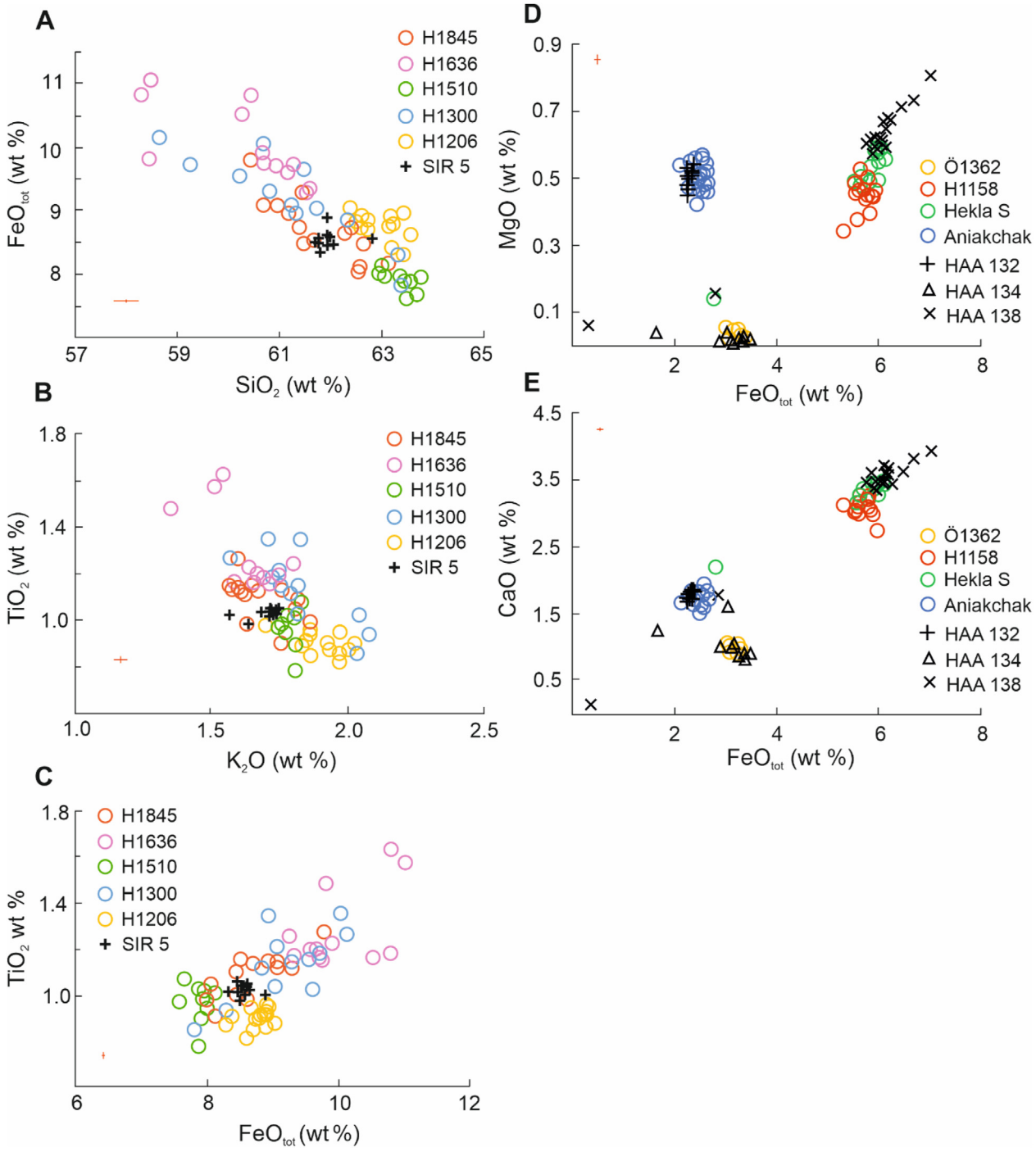


**Fig. 5.** A–C Bivariate plots of major element ratios for glass analyses of selected historical Hekla tephras. Data from Larsen et al. (1999), 2002; Guðmundsdóttir et al. (2016); Kalliokoski et al. (2020). D–E Comparison of three silicic cryptotephras from Haapasuo to published geochemistry of Icelandic and Alaskan tephra. Red cross in the plots represents two standard deviations of repeated analysis of the secondary standards. Data from Larsen et al. (1999); Wastegård et al. (2008); Kaufman et al. (2012); Kalliokoski et al. (2020).

from the deposits at 218–219 cm and 225–226 cm depths due to small shard size. The EMPA results of three of the cryptotephras at this site (Askja, 1875; Hekla 1510 and Hekla 1158) have already been published (Kalliokoski et al., 2020), but all the EMPA data for the remaining nine deposits are given in Table S1. Seven of the cryptotephras at Kivihypönneva are rhyolitic, one is dacitic and one trachydacitic. One cryptotephra layer has an andesitic, and one an andesitic-dacitic composition. One of the cryptotephra deposits (at 89–90 cm depth) consists of a mixture of rhyolitic shards with geochemical signature of several Icelandic volcanic systems.

### 3.2.6. Pervarvikonneva (6)

In the 275 cm long peat core from Pervarvikonneva, seven cryptotephra deposits were identified, at depths of 25–26 cm, 60–61 cm, 65–66 cm, 66–67 cm, 69–70 cm, 115–116 cm and 145–146 cm (Fig. 6A–F in Appendix 1) and geochemical

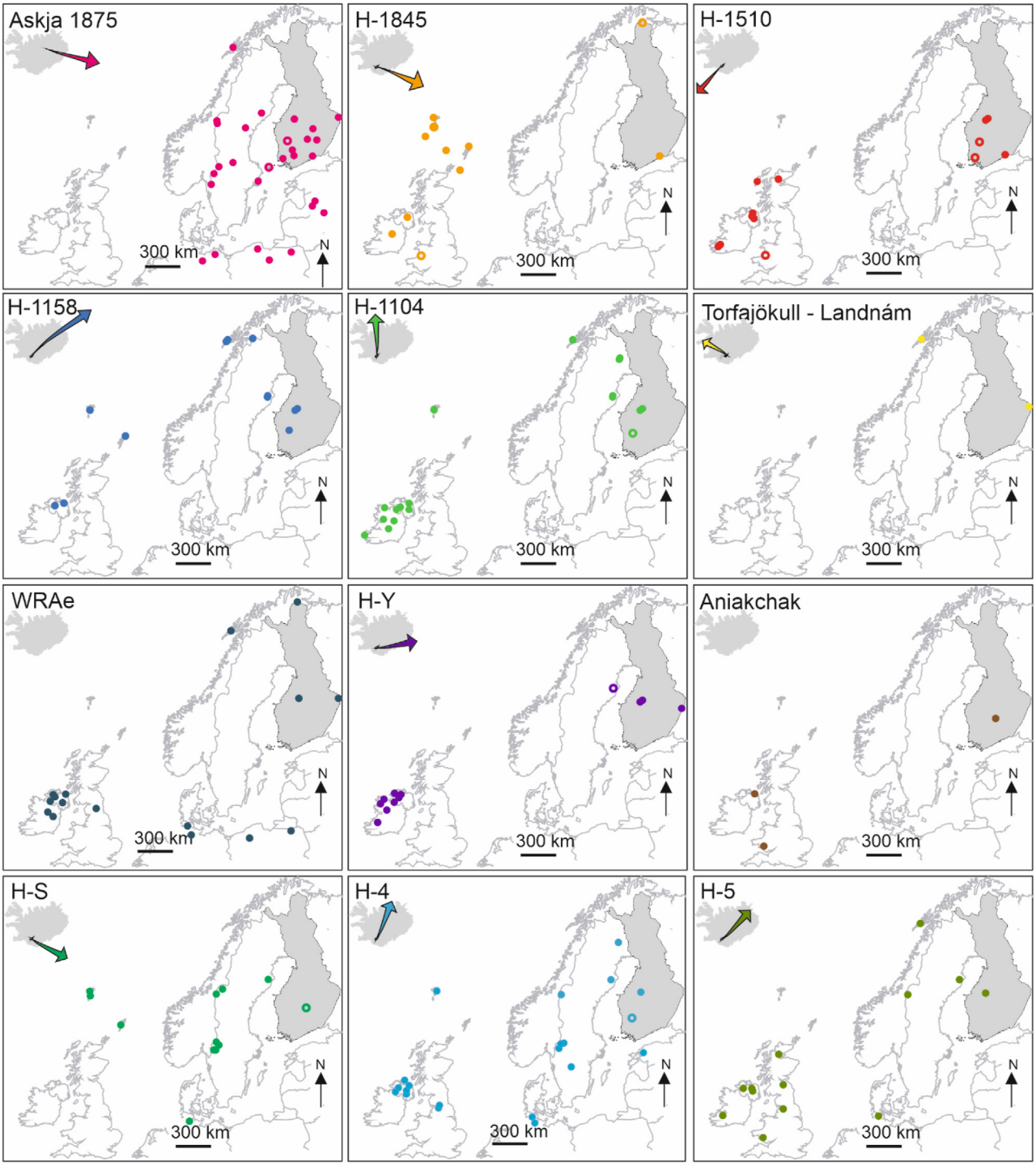


**Fig. 6.** Occurrence maps of cryptotephras detected in Finland. Circles denote tentative correlations. Data sources: Dugmore et al. (1995); Pilcher and Hall (1996); Pilcher et al. (1996); Boygle (1998), 2004; Hall and Pilcher (2002); van den Bogaard and Schmincke (2002); Zillén et al., 2002; Bergman et al. (2004); Plunkett et al. (2004); Pilcher et al. (2005); Plunkett (2006); Davies et al. (2007); Wastegård et al. (2008), 2018; Olsen et al. (2010); Stivrins et al. (2016); Tylmann et al. (2016); Watson et al. (2016), 2017a, 2017b; Wulf et al. (2016); Plunkett and Pilcher (2018); Jones et al. (2019); Swindles et al. (2019); Kinder et al. (2020).

fingerprinting of six of them succeeded (Tables 2 and S1). EMPA results for two of these tephra layers – Hekla 1510 and Hekla 1158 – have been already published. Of the remaining four layers, three originate from Hekla and one from Mt. Churchill in Alaska (Fig. 2).

### 3.2.7. Haapasuo (7)

The 319-cm-thick peat stratigraphy of Haapasuo contains five cryptotephra deposits, at 55–56 cm, 86–89 cm, 132–134 cm, 134–136 cm and 138–140 cm depth. (Fig. 7A–E in Appendix 1). Additionally, brown basaltic shards are present in each centimetre of the 130–140 cm interval. The uppermost tephra has already earlier been assigned to the Askja 1875 eruption, but the geochemical results for the rest of the cryptotephra deposits are published here for the first time (Tables 2 and S1).

### 3.2.8. Kananiemensuo (8)

Seven cryptotephra deposits were detected in the 545-cm-long peat core from Kananiemensuo (Fig. 8A–F in Appendix 1). Three of these (Askja, 1875 at 40–41 cm depth, Hekla, 1845 at 45–46 cm depth and Hekla 1510 at 90–91 cm depth) have been geochemically characterized already earlier, and EMPA has not yet been attempted on the remaining four older deposits at 165–175 cm, 290–300 cm, 345–355 cm and 400–405 cm depths.

### 3.2.9. Tarilampi (9)

The 238-cm-thick peat stratigraphy of Tarilampi contains at least two separate cryptotephra deposits (Fig. 9A–C in Appendix 1) the younger one of which (at 29–30 cm depth) has been correlated to Askja 1875 eruption. Preparation of an EMPA sample failed for the older deposit (at 130–140 cm depth) that consists of colourless platy shards.

### 3.2.10. Punkaharju (10)

In the 660-cm-long peat core from Punkaharju three stratigraphically discrete cryptotephra deposits were detected at 20–30 cm, 415–425 cm and 542–543 cm depths (Fig. 10A and B in Appendix 1). Due to the very small size of shards, EMPA was successful on just one of these deposits, a rhyolitic tephra at 542–543 cm depth, and even for that layer results were obtained from only two shards.

### 3.2.11. Parkusuo (11)

In the 415-cm-long peat core from Parkusuo, two cryptotephra deposits were detected (Fig. 11A in Appendix 1). Of these, the andesitic-dacitic upper layer, at 95–96 cm depth, was geochemically characterized, whereas EMPA of the deposit at 270–280 cm depth failed due to scarce shards that were accidently polished away during EMPA sample preparation.

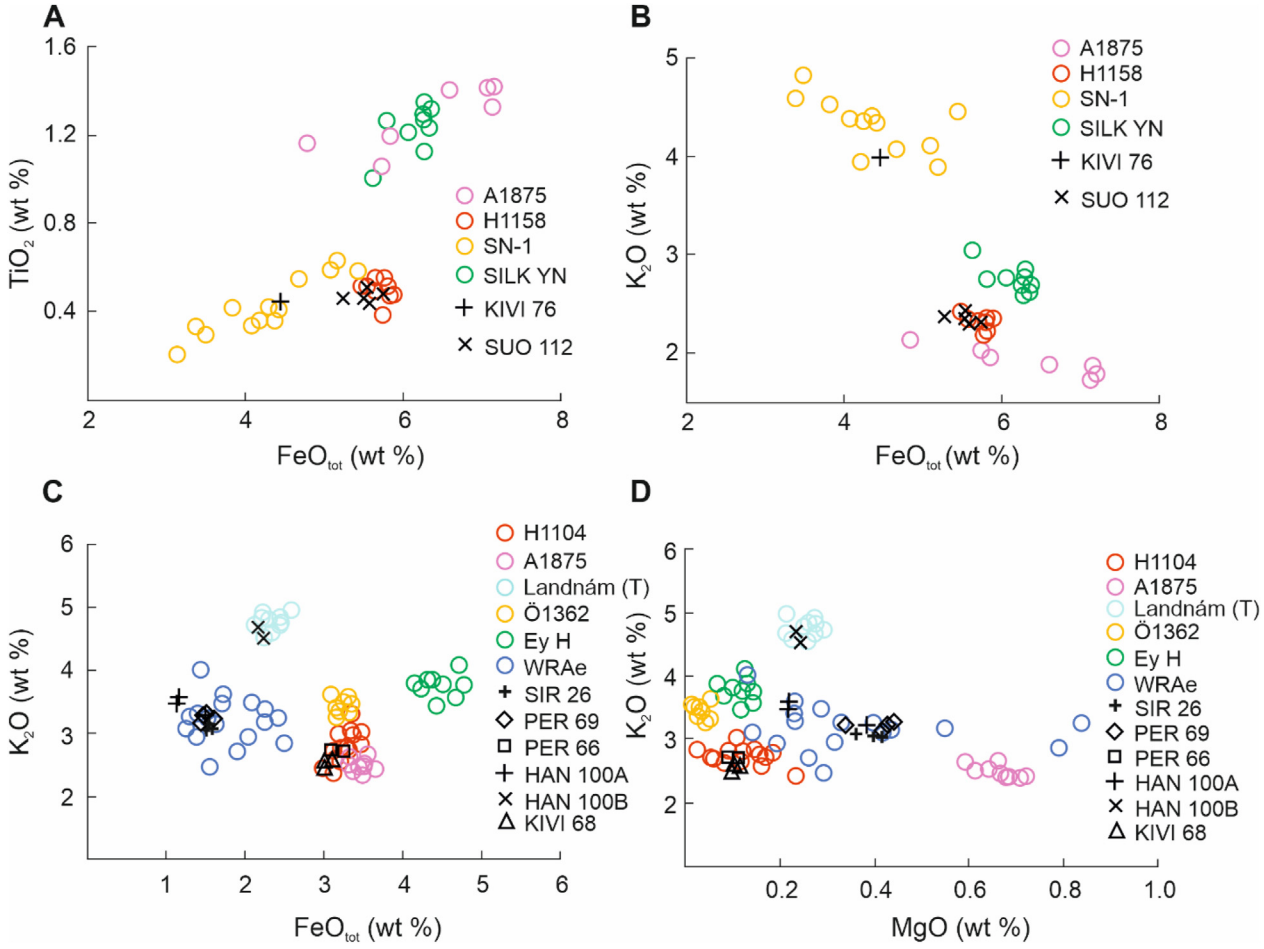


**Fig. 7.** A–B Comparison of analyses of glass from cryptotephra deposits at Kivihypönneva and Suovanalanen to geochemical composition of glass from Icelandic dacitic tephra. Data from Larsen et al. (1999), 2001, 2002; Guðmundsdóttir et al. (2018); Kalliokoski et al. (2019). C–D. Comparison of selected major element ratios of rhyolitic glass from cryptotephras from Finnish sites with geochemical composition of glass from Icelandic and Alaskan volcanoes. The red error bar in the plots represents two standard deviations of repeated analysis of the secondary standards. Data from Larsen et al. (1999); Dugmore et al. (2013); Jensen et al. (2014).

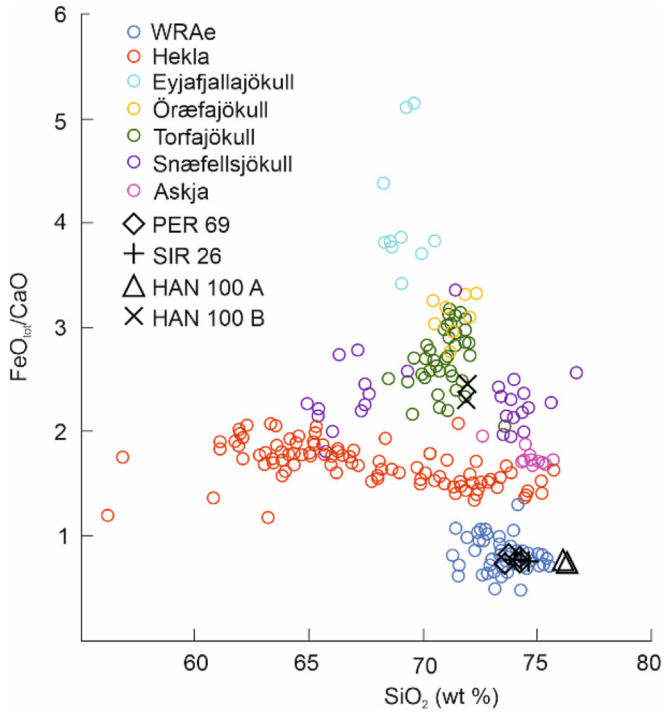


**Fig. 8.** Comparison of the $FeO_{tot}$/CaO ratio of glass from the Torfajökull – Landnám (HAN 100 B) and WRAe cryptotephra (PER 69, SIR 26 and HAN 100 A) in Finland against reference material of the WRAe tephra (Jensen et al., 2014) and Icelandic volcanoes (Boygle, 1999; Larsen et al., 1999, 2002; Óladóttir et al., 2011a; 2011b; Guðmundsdóttir et al., 2011b). The red error bar in the plot represents two standard deviations of repeated analysis of the secondary standards.

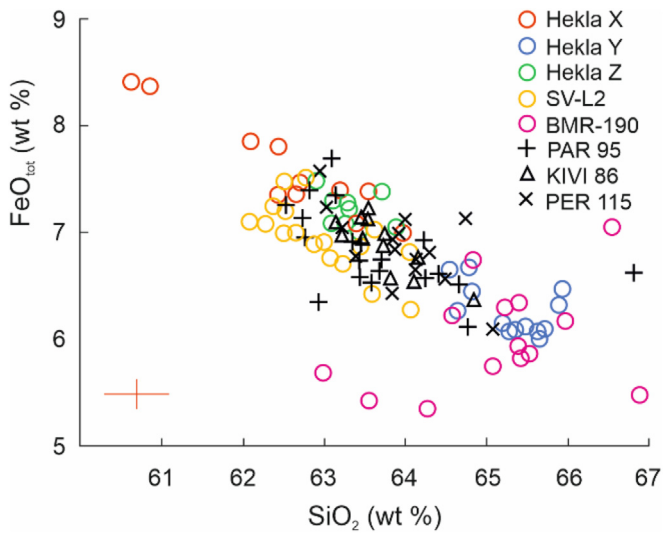


**Fig. 9.** Comparison of analysis of glass shards from cryptotephra horizons at Finnish sites, one Swedish site (Watson et al., 2016: SV-L2) and one Irish site (Plunkett et al., 2004) with new glass geochemical data of the Hekla X, Y, and Z tephra from proximal records. The red error bar in the diagram represents two standard deviations of repeated analysis of the secondary standards.

### 3.2.12. Hanhisuo (12)

The 312-cm-thick peat stratigraphy of Hanhisuo contains two stratigraphically discrete tephra deposits, at 60–61 cm and 100–105 cm depths, respectively (Fig. 12A and B in Appendix 1). The upper deposit consists of the Askja 1875 tephra, and the lower deposit consists of two separate, rhyolitic tephra populations (Tables 2 and S1).

### 3.2.13. Sirrajärvi (13)

The 206-cm-long lacustrine sediment core from Sirrajärvi contains two peaks in cryptotephra concentration, at 5–6 cm and 26–27 cm depths. These deposits were geochemically characterized (Tables 2 and S1). Additionally, sporadic shards of volcanic glass were detected at 60–65 cm, 70–75 cm and 100–105 cm depths, but no EMPA results were obtained from these yet.

## 3.3. Radiocarbon dating

The radiocarbon dating results are given in Table 3 and an age-depth model for Kivihypönneva is shown in Fig. 4.

# 4. Discussion

## 4.1. Geochemically identified cryptotephras in Finland

As mentioned in section 3.2, 37 cryptotephra deposits of a total of 61 were geochemically characterized from Finnish environmental records. Thirty-seven tephra layers were correlated to source volcano/volcanic system and 27 to a specific event. Two different volcanic regions have produced tephra that has reached Finland, and the cryptotephra in Finnish deposits originates from nine volcanoes/volcanic systems and at least 19 separate events. Most of the analysed glass shards in the cryptotephras is intermediate to rhyolitic, but also basaltic volcanic glass originating from three Icelandic volcanic systems is present at one peatland site in central Finland.

### 4.1.1. Askja 1875

The Askja 1875 cryptotephra has been previously identified at nine sites in Finland, and in this study, we suggest a likely occurrence of the Askja 1875 tephra at two additional sites, Stormossen and Suovanalanen (Fig. 2 and Figs. 1A and 4 A in Appendix 1). Askja 1875 tephra is the most common cryptotephra layer at the Finnish sites (Fig. 2). It differs from other cryptotephras present in Finland based on its highly silicic nature, high $TiO_2$ content and larger grain-size, which makes its identification relatively straightforward (Kalliokoski et al., 2019, 2020 and Appendix 1). Based on its wide dispersal also in Norway and Sweden (Boygle, 2004; Bergman et al., 2004; Pilcher et al., 2005; Davies et al., 2007; Borgmark and Wastegård, 2008; Carey et al., 2010) the Askja 1875 tephra carries great potential for becoming an important dating horizon for research focusing on the environmental change of the past 200 years in Fennoscandia.

### 4.1.2. Hekla 1845

Hekla 1845 tephra has been previously identified at our southernmost research site, Kananiemensuo, in southern Finland (Fig. 1). In this study, the upper tephra layer in Sirrajärvi (SIR 5) was found to have a similar andesitic composition as the Hekla 1845 and other historical Hekla tephras, as is demonstrated on bivariate plots of major element ratios (Fig. 5A–C). The full major element geochemistry does not clearly place this tephra in any of the envelopes of the historical Hekla tephras, even if it bears strongest resemblance to the Hekla 1845 tephra (Fig. 5A–C). The Hekla 1845 was a moderate-sized eruption (Volcanic Explosivity Index 4) that produced 0.13 $km^3$ of tephra as loose material (Guðnason et al., 2018). Presence of the Hekla 1845 cryptotephra in the northernmost part of Finland would be surprising, considering the size of the eruption, the east-southeasterly dispersal axis of the tephra in

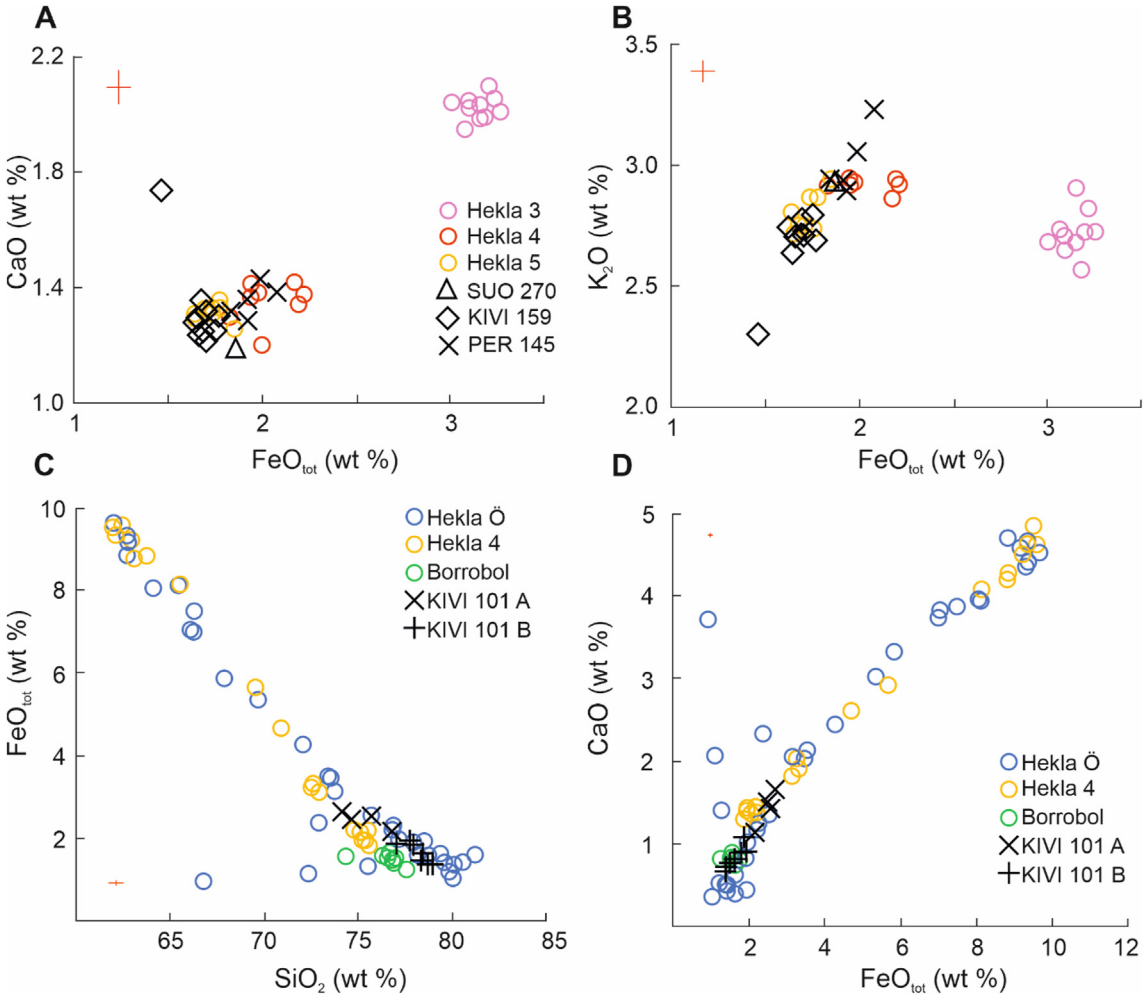


**Fig. 10.** Comparisons of glass analysis of rhyolitic tephra from Finnish sites with proximal glass analytical data of mid-Holocene Hekla tephra. A–B. The red error bar in the plots represents two standard deviations of repeated analysis of the secondary standards. Data from Eiríksson et al. (2004); Óladóttir (2009); Guðmundsdóttir et al. (2016). C–D Data from Turney et al. (1997); Óladóttir (2009).

**Table 3**
Radiocarbon ages for the peat samples from Finnish sites, and for mid-Holocene Öræfajökull tephra in Vopnafjörður, NE Iceland.

| Site/tephra layer | Sample depth (cm) | Dated material | Laboratory ID | 14C age (BP) | Calibrated age range (2σ) BP | Median age (cal yr BP) |
|---|---|---|---|---|---|---|
| Kivihypönneva/above Stömyren? | 80–82 | Sphagnum sp. | AAR 30738 | 1947 ± 24 | 1752–1980 | 1867 |
| Kivihypönneva/above Hekla Ö | 100–101 | Sphagnum sp. | AAR 30739 | 4887 ± 27 | 5581–5704 | 5643 |
| Kivihypönneva/below Hekla Ö | 103–104 | Bulk peat | AAR 30740 | 4483 ± 30 | 4982–5292 | 5137 |
| Kivihypönneva/Hekla 5 | 160–161 | Sphagnum sp. | AAR 30741 | 6115 ± 34 | 6890–7158 | 7024 |
| Kivihypönneva/Unidentified tephra | 227–228 | Sphagnum sp. | AAR 30742 | 6799 ± 39 | 7576–7690 | 7633 |
| Parkusuo/Hekla Y | 95–96 | Sphagnum sp. | AAR 30743 | 2489 ± 28 | 2440–2724 | 2582 |
| Vopnafjörður/Öræfajökull ca. 3.5 cal ka BP | 43–44 | Wood fragments | AAR 30662 | 3292 ± 27 | 3455–3565 | 3510 |

Iceland (Guðnason et al., 2018 and Fig. 6) as well as its absence from central Finland. In contrast, some of the other historical Hekla eruptions, e.g. the Hekla 1300 and Hekla 1636 eruptions, had northerly, north-easterly tephra transport routes based on the main axes of tephra dispersal in Iceland (Larsen et al., 1999; Janebo et al., 2016). Additionally, a single shard of the Hekla 1300 tephra has been identified in Lofoten, northern Norway (Balascio et al., 2011). However, the shallow occurrence depth of the SIR 5, at 5–6 cm (ca. 20 cm above the ca. 860 CE WRAe tephra), together with its geochemical composition supports a correlation to the Hekla 1845 eruption rather than for example to the Hekla 1300 eruption, when a constant accumulation rate is assumed for the lake sediment.

#### 4.1.3. Hekla 1510

The Hekla 1510 tephra has previously been identified at three Finnish peatland sites and one shard with similar geochemistry was analysed from a cryptotephra deposit at Rehtsuo (Fig. 2). In addition to these four sites, we suggest a possible occurrence of Hekla 1510 cryptotephra at Suovanalanen, where a cryptotephra horizon consisting of brownish shards is positioned below a cryptotephra deposit with Askja 1875 characteristics and above the Hekla 1158 cryptotephra horizon (Figs. 2 and 4B in Appendix 1). Interestingly,

the Hekla 1510 tephra has thus far been identified only in Ireland (e.g. Pilcher et al., 1996), Britain (Dugmore et al., 1995; Housley et al., 2010; Watson et al., 2015) and Finland, where it has a relatively wide dispersal area. No indication of the presence of Hekla 1510 has been reported from northern Germany, Poland or Sweden despite multiple cryptotephra investigations undertaken in the region (e.g. van den Bogaard and Schmincke, 2002; Wastegård, 2005; Wulf et al., 2013, 2016; Watson et al., 2017a; Kinder et al., 2020), which points to complex dispersal patterns and localized fall-out.

#### 4.1.4. Öræfajökull 1362/Öræfajökull ca. 3.5 ka BP?

Tephra of Öræfajökull provenance (HAA 134) was identified at Haapasuo in central Finland (Fig. 2). The only distally transported Öræfajökull tephra reported from Fennoscandia is the Öræfajökull 1362 CE tephra (Pilcher et al., 2005). The Öræfajökull 1362 tephra has a distinct geochemical composition with high NaO content and very low MgO content (<0.05 wt %: Larsen et al., 1999), which makes it easily distinguishable from other historical Icelandic silicic tephras (Table 1 and S1, Fig. 5D and E). However, a historical age for this tephra is excluded based on its occurrence depth at 134 cm, ca. 80 cm below the Askja 1875 tephra, and a stratigraphic position between (and partly mixed into) a tephra of Aniakchak geochemistry (HAA 132, see section 4.1.12) and a Hekla tephra (HAA 138, see section 4.2.1). The widespread Aniakchak tephra has been dated to 3.7 ± 0.2 ka BP (Kaufman et al., 2012) and no tephras with similar geochemistry are known from around 1300 CE. However, another Aniakchak tephra (UA, 1966) dating to ~400 BP has been identified in southwestern Alaska by Kaufman et al. (2012) (see section 4.1.12).

On the other hand, older Öræfajökull eruptions have been reported from Iceland (Larsen and Eiríksson, 2008), and a ca. 3–3.4 ka BP Öræfajökull tephra that has been hitherto known only from a proximal site close to Vatnajökull (Guðmundsson, 1998) was recently found in Vopnafjörður, north-east Iceland (Kalliokoski et al., in preparation). This tephra has nearly identical geochemical composition with the 1362 CE eruption, and according to new $^{14}C$ dating results its age is 3510 ± 55 cal yr BP (Table 3 and Kalliokoski et al., in preparation). In addition, two early to mid-Holocene Öræfajökull cryptotephras have recently been found in Wales (Jones et al., 2019).

Furthermore, the Hekla deposit below the Öræfajökull cryptotephra in Haapasuo fits best within the geochemical envelope of the Hekla-S (ca. 3720 cal yr BP: Wastegård et al., 2008) as shown in Fig. 5D and E (discussion in section 4.2.1). Here we suggest an initial correlation of the HAA 134 tephra to the Öræfajökull ~3.5 ka BP eruption based on its stratigraphic position above the assumed Hekla-S cryptotephra while acknowledging a need for radiocarbon dating the peat stratigraphy in Haapasuo to confirm the connection.

#### 4.1.5. Hekla 1158

Dacitic tephra from the 1158 eruption of Hekla has been previously identified at two sites in west-central Finland. In this study, the Hekla 1158 was found from one additional site – Suovanalanen (SUO 112) – and the dispersal area of this tephra in Finland is extended southwards (Fig. 6). In addition to Hekla, three other Icelandic volcanoes – Katla, Snæfellsjökull and Askja – have produced dacitic tephra during the past two millennia (Larsen et al., 1999, 2001, 2002; Schomacker et al., 2016; Kalliokoski et al., 2019), but the products of these volcanic systems differ clearly from each other on bivariate plots of e.g. FeO:$TiO_2$ and FeO:$K_2O$ (Fig. 7A and B).

#### 4.1.6. Hekla 1104 – H1

We identify the rhyolitic Hekla 1104 tephra at two sites in west-central Finland, at Pervarvikonneva (PER 66) and Kivihypönneva (KIVI 68) (Figs. 2 and 7 C–D). The Hekla 1104 glass has nearly identical geochemistry with glass from the rhyolitic part of the Hekla 3 major marker layer. However, the Hekla 1104 lacks the wide geochemical range encountered in Hekla 3 deposits (Larsen et al., 1999), which may at times aid in separating the two from each other. Generally only deposits with $SiO_2$ 70–74 % wt are known for Hekla 1104 in Iceland (e.g. Larsen et al., 1999; Eiríksson et al., 2000), whereas the Hekla 3 has a $SiO_2$ range of 60–74 % wt (e.g. Óladóttir, 2009; Sverrisdóttir, 2007). In Finland, the Hekla 1104 tephra consists of very small, vesicular, colourless shards that are stratigraphically positioned immediately below the Hekla 1158 tephra. The Hekla 1104 tephra is likely partly mixed into the Hekla 1158 tephra deposits, since.

colourless shards occur together with the brownish shards that make up the Hekla 1158 deposits. However, these colourless shards in the Hekla 1158 samples have not been analysed, because they remained under the sample surface during sanding and polishing due to their smaller size. In addition to the two sites where Hekla 1104 is geochemically identified, unanalysed colourless volcanic glass at Suovanalanen ca. 1 cm below the Hekla 1158 tephra could represent the Hekla 1104 tephra (Fig. 2).

#### 4.1.7. Torfajökull – Landnám (877 ± 2 CE)

Two shards with Torfajökull affinity were analysed from cryptotephra at 100–105 cm depth at Hanhisuo, where they form a sparse deposit (HAN 100 B) together with the WRAe tephra (HAN 100 A). Volcanic glass from Torfajökull has a high $K_2O$ content (>4 % wt: Larsen et al., 1999) which makes its separation from other Icelandic tephras straightforward as shown for example on a bivariate plot of FeO:$K_2O$ (Fig. 7 C–D). We propose that the Torfajökull cryptotephra in Hanhisuo represents the silicic part of the 877 ± 2 CE Landnám-tephra (a revised ice core age in Plunkett et al., 2023) that has been identified previously in Lofoten, northern Norway (Pilcher et al., 2005), and in Greenland ice cores (Grönvold et al., 1995; Zielinski et al., 1997) beyond Iceland.

#### 4.1.8. White River Ash - WRAe

This colourless tephra is present at three sites, Pervarvikonneva (PER 69), Hanhisuo (HAN 100 A) and Sirrajärvi (SIR 26), in central and northern Finland. It has a relatively high shard concentration (40 shards/$cm^3$) in the northernmost site, Sirrajärvi. Obtaining robust EMPA results from the shards is, however, difficult due to small shard size and the vesicular nature of the glass (Fig. 13B in Appendix 1). Based on geochemical composition this tephra is the White River Ash originating from the Alaskan volcano Mt. Churchill (Fig. 7C and D and 8). The main diagnostic feature of this tephra is its low FeO:CaO (<1), which separates it from the Icelandic silicic tephras that all have FeO:CaO >1 (Fig. 8). The AD 860 B tephra (e.g. Pilcher et al., 1995; van den Bogaard and Schmincke, 2002; Hall and Pilcher, 2002) has been correlated to the White River Ash eastern lobe by Jensen et al. (2014), which makes it one of the most widely dispersed tephras in northern Europe (e.g. Jensen et al., 2014; Kinder et al., 2020). The age of the WRAe/AD860 B tephra has recently been revised to 852 ± 2 CE (Mackay et al., 2022). The WRAe tephra had not previously been detected in Finland or in the Scandinavian mainland, so these new findings further expand its dispersal area.

#### 4.1.9. SN-1

One volcanic glass grain of Snæfellsjökull provenance was analysed from the depth of 76–78 cm at Kivihypönneva (Fig. 7A and B), where very thin and small (average grain size 38 μm) colourless shards form a scarce cryptotephra deposit (Fig. 5E in Appendix 1). A single analysis alone does not allow for a robust

correlation to be established. However, both the stratigraphic position of this deposit and radiocarbon dating of underlying peat (Fig. 3 and Table 3) support correlation to the SN-1 tephra that was produced by an eruption of Snæfellsjökull in ca. 170 CE (Larsen et al., 2002). SN-1 tephra has been reported previously from northern Sweden (Watson et al., 2016) ca. 400 km north-northwest of Kivihypönneva. An alternative origin in a younger Snæfellsjökull eruption has been suggested for the Swedish deposit (Plunkett and Pilcher, 2018). However, based on our age-depth model (Fig. 4), we suggest the SN-1 eruption to be the most likely source for the cryptotephra deposit at Kivihypönneva.

#### 4.1.10. Askja – Stömyren?

A rhyolitic layer consisting of small colourless shards is present in Kivihypönneva at 82–83 cm depth (Fig. 2). The geochemical composition of glass from this tephra reveals an origin in the Askja central volcano (Table 2). The $^{14}$C dating of the above lying peat (Table 3) and the age range (1864–2376 cal yr BP) obtained from our age-depth model (Fig. 4) points at a similar age for this tephra as for the Glen Garry/Askja ~2000 cal yr BP (Dugmore and Newton, 1992; Dugmore et al., 1995; Pilcher and Hall, 1996; Barber et al., 2008; Guðmundsdóttir et al., 2016). However, correlation to the Glen Garry/Askja ~2000 cal yr BP tephra can be excluded based on the higher $K_2O$ content (>2.3 % wt) of the Askja tephra at Kivihypönneva, since the $K_2O$ content of the Glen Garry tephra is generally <2 % wt (e.g. Dugmore et al., 1995; Barber et al., 2008). This deposit in Kivihypönneva may represent another Askja tephra of similar age, the Stömyren tephra (ca. 2100 cal yr BP), that has been identified in south central Sweden (Wastegård, 2005). The Stömyren tephra has, however, not been correlated to a source eruption yet.

#### 4.1.11. H–Y

An andesitic Hekla tephra consisting of relatively large shards (average grain size 60–80 μm) is present at three sites in central Finland, Pervarvikonneva (PER 115), Kivihypönneva (KIVI 86) and Parkusuo (PAR 95). We correlate this tephra to the Hekla Y eruption (2532 ± 65 BP: Larsen et al., 2020) based on both its geochemical composition (Fig. 9) and its age (2582 ± 142 cal yr BP: Table 3) that was obtained by $^{14}$C dating the horizon at Parkusuo. Additionally, the Hekla Y eruption was one of the largest Hekla alphabet eruptions and therefore likely to produce a widely dispersed tephra horizon (Larsen et al., 2020). In Iceland, the dispersal axis of the Hekla Y tephra stretches NE-E from Hekla (Larsen et al., 2020) and in Finland it seems to have a northerly dispersal (Fig. 5). This tephra has possibly been analysed before from Lake Svartkälsjärn (cryptotephra layer SV-L2) in Northern Sweden (Figs. 9 and 5), even if a correlation to a source eruption has not yet been established there (Watson et al., 2016). The age estimate for the SV-L2 cryptotephra (2000–2500 BP) is younger than the age of Hekla Y (Watson et al., 2016). A correlation to Hekla Y can, however, not be excluded based on the age estimate, since cryptotephra layers in Svartkälsjärn have been dated only indirectly by comparing their occurrence depth with an age-depth model from an older study of the same lake (Watson et al., 2016). In Ireland, a widely dispersed Hekla tephra (ca. 2595 cal yr BP), BMR-190, has been shown to most likely represent the Hekla Y tephra (Plunkett et al., 2004). The slightly higher $SiO_2$ content (62.94–66.87 % wt) and the relatively low $TiO_2$ and FeO contents (average 0.82 % wt and 6.12 % wt, respectively) of the BMR-190 (Plunkett et al., 2004) reveal a perfect match with the Hekla Y tephra in our new proximal dataset (Fig. 9, Table S1). This correlation indicates that H–Y tephra has potential to become an important isochron in northern European paleoenvironmental research.

#### 4.1.12. Aniakchak

A rhyolitic cryptotephra in Haapasuo (HAA 132) has an identical glass geochemical composition to the ca. 3.7 ka BP Aniakchak tephra (Fig. 5D–E; Kaufman et al., 2012), whose ice-core age has recently been revised to 1628 BCE (3578 BP) by Pearson et al. (2022). This tephra originates from a major eruption of the Alaskan Aniakchak volcano with an estimated eruptive bulk volume of >50 km$^3$ (Miller and Smith, 1987). The Aniakchak tephra has been found in the far-distal field in Newfoundland (Pyne-O'Donnell et al., 2012), in the GRIP, NGRIP and GISP2 ice cores in Greenland (Hammer et al., 2003; Pearce et al., 2004; Coulter et al., 2012; Pearson et al., 2022), as well as in Northern Ireland (Plunkett and Pilcher, 2018) and Wales (Jones et al., 2019). No other distally transported tephras are known from the Aniakchak volcano, but in southwestern Alaska younger tephra deposits (3.1 ka BP and 0.4 ka BP) with identical glass geochemical composition have been identified in lake sediments (Kaufman et al., 2012). Additionally, Ponomareva et al. (2018) report several major and minor peaks of Aniakchak glass above the ~3.6 ka BP primary tephra-fall horizon in a marine core from the Chukchi-Alaskan margin, Arctic Sea. However, it is not clear yet, whether these deposits represent primary fall-out or redeposition of older tephra (Kaufman et al., 2012; Ponomareva et al., 2018). The tephra stratigraphy at Haapasuo is problematic due to a lack of radiocarbon dates and the presence of an Öræfajökull tephra immediately below and partly mixed into the Aniakchak tephra (see section 4.1.4). Since some of the Öræfajökull tephras may still be missing from the proximal record in Iceland and the primary vs. secondary nature of some of the Aniakchak tephras need yet to be determined, we refrain from suggesting definite correlations to source eruptions for the cryptotephra deposits in Haapasuo at this stage.

#### 4.1.13. Hekla 4 - H4

We have geochemically identified the Hekla 4 tephra in Pervarvikonneva, at the depth of 145–146 cm, where it forms a horizon consisting of small, colourless glass grains. The Hekla 4 can be separated from Hekla 3 and Hekla 5 tephras for example on bivariate plots of FeO:CaO and FeO:$K_2O$ (Fig. 10A and B). The small geochemical differences between Hekla tephras become visible when comparisons are made between samples with similar $SiO_2$ range. The Hekla 4 tephra has been previously identified in several sites in northern Europe and its dispersal area is one of the widest for Holocene tephras (Fig. 6).

#### 4.1.14. Hekla Ö - HÖ

The cryptotephra at the depth of 101–102 cm in Kivihypönneva forms a very clear rhyolitic layer with relatively high shard concentration (175 shards/cm$^3$). It consists of two geochemical populations, KIVI 101 A and KIVI 101 B, the 101 A population being of a typical rhyolitic Hekla composition (Fig. 10C and D), whereas the 101 B population has a very high $SiO_2$ content and geochemical composition that resembles volcanic glass that has occasionally been analysed as a minor component in some of the Hekla deposits in Iceland (e.g. Sigvaldason, 1974; Larsen and Eiríksson, 2008; Óladóttir, 2009). Both populations are here tentatively correlated to the Hekla Ö layer in Iceland, where an identical glass geochemistry has been reported from sites immediately north of Vatnajökull (Óladóttir, 2009). However, since the KIVI 101 B composition is present in Hekla Ö deposits only at a few sites north of Vatnajökull and not found in proximal settings (e.g. Guðmundsdóttir et al., 2011a; Jónsson et al., 2020), these shards may also originate from a different volcanic system (e.g. þórðarhyrna or Torfajökull) that erupted close enough in time for the tephra to form a mixed layer with the Hekla-Ö. The KIVI 101 B population has similar geochemical composition as for example the 14 ka BP Borrobol

(Turney et al., 1997) and the SAU-65 (ca. 2600 cal yr BP: Larsen and Eiríksson, 2008) tephras, whose source volcano is not known (Fig. 10C and D).

In Iceland, the Hekla Ö tephra has been radiocarbon dated to be 6061 ± 136 cal yr BP (Guðmundsdóttir et al., 2011a). Unfortunately, $^{14}C$ dating of the cryptotephra horizon in Kivihypönneva gives contradicting results (Table 3). Radiocarbon ages of peat 1 cm above and below the tephra horizon are reversed (Table 3). The lower age (5137 ± 155 cal yr BP) comes from a bulk sample of peat which possibly contains material of different ages (such as roots), whereas the upper age (5643 ± 62 cal yr BP) was obtained from hand-picked Sphagnum sp. stems and leaves. The upper age is therefore considered more reliable than the bulk peat age and it provides a minimum age for the tephra horizon. The age-depth model (Fig. 4) gives an age range of 5594–5673 cal yr BP for the tephra layer. Since no other Hekla layers with similar geochemical composition are known from this time, we suggest a tentative correlation to the Hekla Ö eruption for this layer despite the dating uncertainties at our site.

#### 4.1.15. Hekla 5 - H5

Hekla 5 tephra (ca 7050 cal yr BP: Thorarinsson, 1971) is identified at Kivihypönneva at the depth of 159–160 cm, where it forms a layer with high shard concentration (400 shards/cm$^3$). Hekla 5 can be separated from the other silicic mid-Holocene Hekla tephras by its highly silicic nature and low FeO content (Fig. 10A and B). Hekla 5 deposits with $SiO_2$ < 73 % wt are not known from Iceland (e.g. Eiríksson et al., 2004; Søndergaard, 2005). Radiocarbon dating gives an age of 7024 ± 134 cal yr BP for this layer at Kivihypönneva (Table 3), which also supports the correlation to Hekla 5.

### 4.2. Uncorrelated silicic tephras

#### 4.2.1. Dacitic cryptotephra HAA 138

Cryptotephra at 138–140 cm depth in Haapasuo (HAA 138) has a geochemical signature of Hekla central volcano (Tables 2 and S1). Most shards are dacitic, but also two rhyolitic shards were analysed (Table S1). Correlating this deposit to a source eruption is challenging, because no radiocarbon dates exist for the peat core and robust correlations have not yet been established for the two cryptotephra horizons, Aniakchak (HAA 132) and Öræfajökull (HAA 134) tephra, above this deposit. This tephra could be correlated either to the Hekla 1158 and Hekla 1104 eruptions, or to the Hekla S tephra (ca. 3720 cal yr BP: Wastegård et al., 2008). Correlation to the Hekla S tephra is more likely due to the lower $K_2O$ content (<2.0 wt %) of this tephra compared to the $K_2O$ content of the Hekla 1158 tephra (≥2.3 wt %) (Fig. 5D and E and Table 2). Further support for this correlation is given by the presence of basaltic glass from the Kverkfjöll central volcano that has not erupted during historical time (Table 2 and section 4.3). However, further investigations are needed for establishing a robust tephrochronology for this site.

#### 4.2.2. Mixed cryptotephra KIVI 89

A sample from the 89–90 cm depth in Kivihypönneva (KIVI 89) contains a mixed tephra population. Only a couple of analyses were obtained from this deposit. One shard has a similar composition as that of the Hekla 3 and Hekla S tephras, whereas the other shows Öræfajökull affinity (Table S1). According to our age-depth model, the age range at this depth is 2704–4363 cal yr BP. The Öræfajökull shard at this depth possibly represents the same volcanic event as the Öræfajökull cryptotephra deposit in Haapasuo (HAA 134).

#### 4.2.3. Two rhyolitic cryptotephras KIVI 218 and KIVI 225

At Kivihypönneva, there are two rhyolitic cryptotephra horizons (KIVI 218 and KIVI 225) below the Hekla 5 tephra. EMPA results from these deposits indicate either a non-Icelandic origin, or erroneous values for some of the major elements (Table S1), possibly due to beam-induced sodium and potassium migration during analysis (e.g. Hunt and Hill, 2001; Hayward, 2012). However, no firm conclusions can be made based on so few analyses. EMPA was attempted on two sets of samples from both horizons, but no further results could be obtained from the thin and small shards. Radiocarbon dating of the peat immediately below the lower horizon gives a maximum age of 7634 ± 57 cal yr BP for the deposits and our age-depth model (Fig. 4) suggests an age of 7456–7610 cal yr BP for KIVI 218, and an age of 7558–7658 cal yr BP for KIVI 225. Further research is needed for geochemical fingerprinting of these cryptotephra deposits.

### 4.3. Basaltic tephras

Basaltic volcanic glass was detected at just one site, Haapasuo, where it forms a diffuse deposit at 130–140 cm depth. The cryptotephra in this deposit can be divided into three populations that show compositional characteristics of the Grímsvötn, Veiðivötn and Kverkfjöll volcanoes, respectively (Tables 2 and S1). Grímsvötn and Veiðivötn have both erupted frequently throughout the Holocene (Óladóttir et al., 2011a), producing basaltic tephras that show only limited compositional variation (Óladóttir et al., 2011b). Kverkjöll, on the other hand, has not erupted during the historical time (Óladóttir et al., 2011a). The ambiguous glass geochemistry together with the diffuse nature of the basaltic cryptotephra deposit at Haapasuo does not allow for tracing the source eruptions of these deposits without better age constraints.

Basaltic cryptotephras have possibly remained undetected at other Finnish sites due to their fine grain-size. The longest axes of the basaltic glass shards in Haapasuo are <30 μm and samples in this study were generally sieved with a 24 μm mesh. A 10 μm mesh was tested just for the Haapasuo core. In general, very few Icelandic basaltic tephras have been identified from the northern European environmental records thus far (e.g. Wastegård and Davies, 2009; Lawson et al., 2012) despite the frequent basaltic explosive eruptions taking place in Iceland (Larsen and Eiríksson, 2008). The highest number of basaltic tephra layers is found in the Faroe Islands, where six basaltic horizons originating from Veiðivötn, Grímsvötn and Kverkfjöll have been identified (Wastegård et al., 2018). In addition to these findings, basaltic Veiðivötn tephra has been identified in Ireland (Chambers et al., 2004) and central Sweden (Davies et al., 2007), and two basaltic cryptotephras, the Laki 1783 (Kekonen et al., 2005) and Grímsvötn 1903 tephra (Wastegård and Davies, 2009), have been discovered in Svalbard, arctic Norway. Additionally, basaltic cryptotephra from three Icelandic volcanic systems, Grímsvötn, Katla and Veiðivötn, has recently been reported from Russia (Vakhrameeva et al., 2020). It is therefore possible, that the Icelandic basaltic cryptotephras may generally have a more northerly dispersal than their silicic counterparts, and the lack of basaltic tephras in the northern European tephra framework may partly reflect the scarcity of cryptotephra research conducted in northern Fennoscandia as well.

### 4.4. Challenges of cryptotephra studies in Finland

Several cryptotephra horizons remain still unanalysed due to many of the deposits consisting of very small and scarce volcanic shards that present challenges for EMPA. Additionally, some of the deposits could not be confidently assigned to source eruptions, because geochemical characterization succeeded only for a few shards despite several attempts at preparing new samples from the same depth. A low number of analyses per cryptotephra deposit does not enable a critical assessment of the quality of the EMPA

results, thus, more research needs to be conducted at some of the sites before suggesting firmer correlations to source eruptions. Additionally, the difficulties in comparing more and less evolved Hekla tephra erupted from a zoned magma chamber during the same volcanic event (e.g. Larsen and Thorarinsson, 1977; Sigmarsson et al., 1992; Jónsson et al., 2020) become accentuated in the ultra-distal area, where the number of tephra shards suitable for EMPA is generally low and results rarely cover the full range of erupted products. Furthermore, small shard size and the common presence of microlites in the vesicular (andesitic) Hekla tephra (Hunt and Hill, 2001; Lowe et al., 2017) make obtaining analysis of pure glass demanding. Thus, minor differences between compositions of individual Hekla tephras may sometimes remain obscure due to accidental analysis of microcrystals, or low analysis totals. To confirm the origin of some of the deposits in Finland, further research and using additional dating methods is necessary. The refined tephra dispersal maps of several Icelandic Holocene eruptions (Fig. 6) confirm that the proximal dispersal axis of tephra can often not be used as an aid in determining which cryptotephras are likely to be present in the distal region. For example, the occurrence of several Hekla tephras (H-1510, H-1104, H-4 and H-5), and the Torfajökull component of the Landnám tephra in Finland is unexpected based on the orientation of their dispersal axes in Iceland (Fig. 6).

## 5. Conclusions

Cryptotephra investigation at 13 Finnish sites reveals the presence of at least 19 geochemically distinct Holocene cryptotephras of Icelandic and Alaskan origin. Fifteen of these tephras were found in Finland for the first time in this study. The first correlation of ultra-distal Hekla Y deposits to their counterparts in Iceland based on new geochemical results of glass analyses from proximal records, as well as the first tentative identification of Öræfajökull 3.5 ka BP tephra outside of Iceland, highlight the benefits of conducting research simultaneously both in the proximal and distal region. The oldest geochemically characterized cryptotephra in the Finnish environmental records is the ca. 7 ka BP Hekla 5 tephra and the youngest is the Askja 1875. These results demonstrate that tephra has traveled to Finland frequently during the Holocene, and there is an excellent potential for using tephrochronology as a dating method in environmental studies in the region. Additionally, the identification of two Alaskan tephras – the WRAe and Aniakchak tephra – in Finland reveal an opportunity for intercontinental linking of environmental archives. The majority of the cryptotephra deposits in Finnish environmental records consist of scarce and small shards, and geochemical fingerprinting of the deposits requires rigorous laboratory methods and often repeated analysis attempts at the electron microprobe. Despite these methodological and analytical challenges, simultaneous investigation of several sites both in Finland and Iceland has allowed us to construct a first outline for a Finnish tephrochronology, which serves as an initial framework that can be expanded and refined by future cryptotephra research in Finland and nearby regions.

## Credit author statement

Maarit Kalliokoski: Investigation, Methodology, Writing – Original draft, Writing – Review & Editing, Project administration, Funding acquisition, Conceptualization, Visualization, Esther Ruth Guðmundsdóttir: Writing – Review & Editing, Stefan Wastegård: Writing – Review & Editing, Supervision, Sami Jokinen: Formal analysis, Timo Saarinen: Conceptualization, Writing – Review & Editing.

## Declaration of competing interest

The authors declare that they have no known competing financial interests or personal relationships that could have appeared to influence the work reported in this paper.

## Data availability

All the data is available in the supplementary files

## Acknowledgements

We thank Dr Maria Janebo for assistance with field work in Iceland and Kari Kalliokoski for help with field work in Finland. This work was funded by the Nordic Volcanological Centre at the University of Iceland, the Finnish Cultural Foundation, Varsinais-Suomi Regional Fund, and the Academy of Finland (grant no. 339789).

## Appendix A. Supplementary data

Supplementary data to this article can be found online at https://doi.org/10.1016/j.quascirev.2023.108173.

## References

Balascio, N.L., Wickler, S., Narmo, L.E., Bradley, R.S., 2011. Distal cryptotephra found in a Viking boathouse: the potential for tephrochronology in reconstructing the Iron Age in Norway. J. Archaeol. Sci. 38, 934–941.
Barber, K., Langdon, P., Blundell, A., 2008. Dating the Glen Garry tephra: a widespread late-Holocene marker horizon in the peatlands of northern Britain. Holocene 18, 31–43.
Bergman, J., Wastegård, S., Hammarlund, D., Wohlfarth, B., Roberts, S.J., 2004. Holocene tephra horizons at Klocka Bog, west-central Sweden: aspects of reproducibility in subarctic peat deposits. J. Quat. Sci. 19, 241–249.
Björck, S., Ingólfsson, Ó., Hafliðason, H., Hallsdóttir, M., Anderson, N.J., 1992. Lake Torfadalsvatn: a high resolution record of the North Atlantic ash zone I and the last glacial-interglacial environmental changes in Iceland. Boreas 21, 15–22.
Blockley, S.P.E., Pyne-O'Donnell, S.D.F., Lowe, J.J., Matthews, I.P., Stone, A., Pollard, A.M., Turney, C.S.M., Molyneux, E., 2005. A new and less destructive laboratory procedure for the physical separation of distal glass tephra shards from sediments. Quat. Sci. Rev. 24, 1952–1960.
Borgmark, A., Wastegård, S., 2008. Regional and local patterns of peat humification in three raised peat bogs in Värmland, south-central Sweden. GFF 130, 161–176.
Boygle, J., 1998. A little goes a long way: discovery of a new mid Holocene tephra in Sweden. Boreas 27, 195–199.
Boygle, J., 1999. Variability of tephra in lake and catchment sediments, Svínavatn, Iceland. Global Planet. Change 21, 129–149.
Boygle, J., 2004. Towards a Holocene tephrochronology for Sweden: geochemistry and correlation with the North Atlantic tephra stratigraphy. J. Quat. Sci. 19, 103–109.
Bronk Ramsey, C., 2009. Bayesian analysis of radiocarbon dates. Radiocarbon 51, 337–360.
Carey, R.J., Houghton, B.F., Thordarson, T., 2010. Tephra dispersal and eruption dynamics of wet and dry phases of the 1875 eruption of Askja volcano, Iceland. Bull. Volcanol. 72, 259–278.
Chambers, F.M., Daniell, J.R.G., Hunt, J.B., Molloy, K., O'Connell, M., 2004. Tephrostratigraphy of an Loch Mór, Iniss Oírr, western Ireland: implications for Holocene tephrochronology in the northeastern Atlantic region. Holocene 14, 703–720.
Cooper, C.L., Swindles, G.T., Watson, E.J., Savov, I.P., Gałka, M., Gallego-Sala, A., Borken, W., 2019a. Evaluating tephrochronology in the permafrost peatlands of northern Sweden. Quat. Geochronol. 50, 16–28.
Cooper, C.L., Savov, I.P., Swindles, G.T., 2019b. Standard chemical-based tephra extraction methods significantly alter the geochemistry of volcanic glass shards. J. Quat. Sci. 34, 697–707.
Coulter, S.E., Pilcher, J.R., Plunkett, G., Baillie, M., Hall, V.A., Steffensen, J.P., Vinther, B.M., Clausen, H.B., Johnsen, S.J., 2012. Holocene tephras highlight complexity of volcanic signals in Greenland ice cores. J. Geophys. Res. 117, D21303. https://doi.org/10.1029/2012JD017698.
Davies, S.M., 2015. Cryptotephras: the revolution in correlation and precision dating. J. Quat. Sci. 30, 114–130.
Davies, S.M., Elmquist, M., Bergman, J., Wohlfarth, B., Hammarlund, D., 2007. Cryptotephra sedimentation processes within two lacustrine sequences from west central Sweden. Holocene 17, 319–330.
Dugmore, A.J., 1989. Icelandic volcanic ash in Scotland. Scot. Geogr. Mag. 105, 168–172.
Dugmore, A.J., Newton, A.J., 1992. Thin tephra layers in peat revealed by X-

radiography. J. Archaeol. Sci. 19, 163–170.
Dugmore, A.J., Larsen, G., Newton, A.J., 1995. Seven tephra isochrones in Scotland. Holocene 5, 257–266.
Dugmore, A.J., Newton, A.J., Smith, K.T., Mairs, K.-A., 2013. Tephrochronology and the late Holocene volcanic and flood history of Eyjafjallajökull, Iceland. J. Quat. Sci. 28, 237–247.
Eiríksson, J., Knudsen, K.L., Haflidason, H., Heinemeier, J., 2000. Chronology of late Holocene climatic events in the northern North Atlantic based on AMS 14C dates and tephra markers from the volcano Hekla, Iceland. J. Quat. Sci. 15, 573–580.
Eiríksson, J., Larsen, G., Knudsen, K.L., Heinemeier, J., Símonarson, L.A., 2004. Marine reservoir age variability and water mass distribution in the Iceland Sea. Quat. Sci. Rev. 23, 2247–2268.
Grönvold, K., Óskarsson, N., Johnsen, S.J., Clausen, H.B., Hammer, C.U., Bond, G., Bard, E., 1995. Ash layers from Iceland in the Greenland GRIP ice core correlated with oceanic and land sediments. Earth Planet Sci. Lett. 135, 149–155.
Guðmundsdóttir, E.R., Larsen, G., Eiríksson, J., 2011a. Two new Icelandic tephra markers: the Hekla Ö tephra layer, ~6060 cal. yr BP, and Hekla DH tephra layer, ~6650 cal. yr. BP. Land-sea correlation of mid-Holocene tephra markers. Holocene 21, 629–639.
Guðmundsdóttir, E.R., Eiríksson, J., Larsen, G., 2011b. Identification and definition of primary and reworked tephra in Late Glacial and Holocene marine shelf sediments off North Iceland. J. Quat. Sci. 26, 589–602.
Guðmundsdóttir, E.R., Larsen, G., Björck, S., Ingólfsson, Ó., Striberger, J., 2016. A new high-resolution Holocene tephra stratigraphy in eastern Iceland: improving the Icelandic and North Atlantic tephrochronology. Quat. Sci. Rev. 150, 234–249.
Guðmundsdóttir, E.R., Schomacker, A., Brynjólfsson, S., Ingólfsson, Ó., Larsen, N.K., 2018. Holocene tephrostratigraphy in vestfirðir, NW Iceland. J. Quat. Sci. 33, 827–839.
Guðmundsson, H., 1998. Holocene Glacier Fluctuations and Tephrochronology of the Öræfi District, Iceland. PhD Thesis. University of Edinburgh, Edinburg.
Guðnason, J., Thordarson, T., Houghton, B.F., Larsen, G., 2018. The 1845 Hekla eruption: grain-size characteristics of a tephra layer. J. Volcanol. Geoth. Res. 350, 33–46.
Haflidason, H., Eiriksson, J., Van Kreveld, S., 2000. The tephrochronology of Iceland and the north atlantic region during the middle and late quaternary: a review. J. Quat. Sci. 15, 3–22.
Haflidason, H., Regnéll, C., Pyne-O'Donnell, S., Svendsen, J.I., 2019. Extending the known distribution of the vedde ash into siberia: occurrence in lake sediments from the timan ridge and the ural mountains, northern Russia. Boreas 48, 444–451.
Hall, V.A., Pilcher, J.R., 2002. Late-Quaternary Icelandic tephras in Ireland and Great Britain: detection, characterization and usefulness. Holocene 12, 223–230.
Hammer, C.U., Kurat, G., Hoppe, P., Grum, W., Clausen, H.B., 2003. The eruption date 1645BC confirmed by new ice core data). In: Bietak, M. (Ed.), The Synchronisation of Civilisations in the Eastern Mediterranean in the Second Millennium B.C. Proceedings of the SCIEM 2000 – EuroConference Haindorf. Osterreichischen Akad. der Wiss., Vienna, pp. 87–93.
Harning, D.J., Thordarson, T., Geirsdóttir, Á., Zalzal, K., Miller, G.H., 2018. Provenance, stratigraphy and schronology of Holocene tephra from Vestfirðir, Iceland. Quat. Geochronol. 46, 59–76.
Hayward, C., 2012. High spatial resolution electron probe microanalysis of tephras and melt inclusions without beam-induced chemical modification. Holocene 22, 119–125.
Housley, R.A., Blockley, S.P.E., Matthews, I.P., MacLeod, A., Lowe, J.J., Ramsay, S., Miller, J.J., Campbell, E.N., 2010. Late Holocene vegetation and palaeoenvironmental history of the Dunadd area, Argyll, Scotland: chronology of events. J. Archaeol. Sci. 37, 577–593.
Housley, R.A., MacLeod, A., Nalepka, D., Jurochnik, A., Masojć, M., Davies, L., Lincoln, P.C., Bronk Ramsey, C., Gamble, C.S., Lowe, J.J., 2013. Tephrostratigraphy of a Lateglacial lake sediment sequence at Węgliny, southwest Poland. Quat. Sci. Rev. 77, 4–18.
Hunt, J.B., Hill, P.G., 2001. Tephrological implications of beam size–sample-size effects in electron microprobe analysis of glass shards. J. Quat. Sci. 16, 105–117.
Janebo, M.H., Thordarson, T., Houghton, B.F., Bonadonna, C., Larsen, G., Carey, R.J., 2016. Dispersal of key subplinian–Plinian tephras from Hekla volcano, Iceland: implications for eruption source parameters. Bull. Volcanol. 78, 66.
Jensen, B.J.L., Pyne O'Donnell, S., Plunkett, G., Froese, D.G., Hughes, P.D.M., Sigl, M., McConnell, J.R., Amesbury, M.J., Blackwell, P.G., van den Bogaard, C., Buck, C.E., Charman, D.J., Clague, J.J., Hall, V.A., Koch, J., Mackay, H., Mallon, G., McColl, L., Pilcher, J.R., 2014. Transatlantic distribution of the alaskan White River Ash. Geology 42, 875–878.
Johansson, H., Lind, E.M., Wastegård, S., 2017. Compositions of glass in proximal tephras from eruptions in the Azores archipelago and their links with distal sites in Ireland. Quat. Geochronol. 40, 120–128.
Jones, G., Davies, S.M., Farr, G.J., Bevan, J., 2017. Identification of the Askja-S tephra in a rare turlough record from pant-y-llyn, south Wales. PGA (Proc. Geol. Assoc.) 128, 523–530.
Jones, G., Davies, S.M., Staff, R.A., Loader, N.J., Davies, S.J., Walker, M.J.C., 2019. Traces of volcanic ash from the mediterranean, Iceland and north America in a Holocene record from south Wales, UK. J. Quat. Sci. 35, 163–174.
Jónsson, D.F., Gudmundsdóttir, E.R., Larsen, G., Óladóttir, B.A., Erlendsson, E., Eddudóttir, S.D., Sigmarsson, O., 2020. The multi-component Hekla Ö Tephra, Iceland: a complex widespread mid-Holocene tephra layer. J. Quat. Sci. 35, 410–421.
Kalliokoski, M., Wastegård, S., Saarinen, T., 2019. Rhyolitic and dacitic component of the Askja 1875 tephra in southern and central Finland: first step towards a Finnish tephrochronology. J. Quat. Sci. 34, 29–39.
Kalliokoski, M., Guðmundsdóttir, E.R., Wastegård, S., 2020. Hekla 1947, 1845, 1510 and 1158 tephra in Finland: challenges of tracing tephra from moderate eruptions. J. Quat. Sci. 35, 803–816.
Kaufman, D.S., Jensen, B.J.L., Reyes, A.V., Schiff, C.J., Froese, D.G., Pearce, N.J.G., 2012. Late quaternary tephrostratigraphy, ahklun mountains, SW Alaska. J. Quat. Sci. 27, 344–359.
Kekonen, T., Moore, J., Perämäki, P., Martma, T., 2005. The Icelandic Laki volcanic tephra layer in the Lomonosovfonna ice core, Svalbard. Polar Res. 24, 33–40.
Kinder, M., Wulf, S., Appelt, O., Hardiman, M., Żarczyński, M., Tylmann, W., 2020. Late-Holocene ultra-distal cryptotephra discoveries in varved sediments of Lake Żabińskie, NE Poland. J. Volcanol. Geoth. Res. 402, 106988.
Lane, C.S., Cullen, V.L., White, D., Bramham-Law, C.W.F., Smith, V.C., 2014. Cryptotephra as a dating and correlation tool in archaeology. J. Archaeol. Sci. 42, 42–50.
Larsen, G., Eiríksson, J., 2008. Late Quaternary terrestrial tephrochronology of Iceland – frequency of explosive eruptions, type and volume of tephra deposits. J. Quat. Sci. 23, 109–120.
Larsen, G., Thorarinsson, S., 1977. H4 and other acid Hekla layers. Jokull 27, 28–46.
Larsen, G., Dugmore, A., Newton, A., 1999. Geochemistry of historical-age silicic tephras in Iceland. Holocene 9, 463–471.
Larsen, G., Newton, A.J., Dugmore, A.J., Vilmundardóttir, E., 2001. Geochemistry, dispersal, volumes and chronology of Holocene silicic tephra layers from the Katla volcanic system, Iceland. J. Quat. Sci. 16, 119–132.
Larsen, G., Eiríksson, J., Knudsen, K.L., Heinemeier, J., 2002. Correlation of late Holocene terrestrial and marine tephra markers, north Iceland: implications for reservoir age changes. Polar Res. 21, 283–290.
Larsen, G., Róbertsdóttir, B.G., Óladóttir, B.A., Eiríksson, J., 2020. A shift in eruption mode of Hekla volcano, Iceland, 3000 years ago: two-coloured Hekla tephra series, characteristics, dispersal and age. J. Quat. Sci. 35, 143–154.
Lawson, I.T., Swindles, G.T., Plunkett, G., Greenberg, D., 2012. The spatial distribution of Holocene cryptotephras in north-west Europe since 7 ka: implications for understanding ash fall events from Icelandic eruptions. Quat. Sci. Rev. 41, 57–66.
Lougheed, B.C., Obrochta, S.P., 2019. A rapid, deterministic age-depth modeling routine for geological sequences with inherent depth uncertainty. Paleoceanogr. Paleoclimatol. 34, 122–133.
Lowe, D.J., 2011. Tephrochronology and its applications: a review. Quat. Geochronol. 6, 107–153.
Lowe, D.J., Pearce, N.J.G., Jorgensen, M.A., Kuehn, S.C., Tryon, C.A., Hayward, C.L., 2017. Correlating tephras and cryptotephras using glass compositional analyses and numerical and statistical methods: review and evaluation. Quat. Sci. Rev. 175, 1–44.
MacLeod, A., Brunnberg, L., Wastegård, S., Hang, T., Matthews, I.P., 2014. Lateglacial cryptotephra detected within clay varves in Östergötland, south-east Sweden. J. Quat. Sci. 29, 605–609.
Mackay, H., Plunkett, G., Jensen, B.J.L., Aubry, T.J., Corona, C., Kim, W.M., Toohey, M., Sigl, M., Stoffel, M., Anchikaitis, K.J., Raible, C., Bolton, M.S.M., Manning, J.G., Newfield, T.P., Di Cosmo, N., Ludlow, F., Kostick, C., Yang, Z., Coyle McClung, L., Amesbury, M., Monteath, A., Hughes, P.D.M., Langdon, P.G., Charman, D., Booth, R., Davies, K.L., Blundell, A., Swindles, G.T., 2022. The 852/3 CE Mount Churchill eruption: examining the potential climatic and societal impacts and the timing of the Medieval Climate Anomaly in the North Atlantic region. Clim. Past 18, 1457–1508.
Meara, R.H.H., Thordarson, T.H., Pearce, N.J.G., Hayward, C., Larsen, G., 2020. A catalogue of major and trace element data for Icelandic Holocene silicic tephra layers. J. Quat. Sci. 35, 122–142.
Miller, T.P., Smith, R.L., 1987. Late Quaternary caldera-forming eruptions in the eastern Aleutian arc, Alaska. Geology 15, 434–438.
Óladóttir, B.A., 2009. Holocene Eruption History and Magmatic Evolution of the Subglacial Vatnajökull Volcanoes, Grímsvötn, Bárdarbunga and Kverkfjöll, Iceland. PhD Thesis, Université Blaise Pascal. Clermont-Ferrand and University of Iceland, Reykjavík.
Óladóttir, B.A., Sigmarsson, O., Larsen, G., Thordarson, T., 2008. Katla volcano, Iceland: magma composition, dynamics and eruption frequency as recorded by Holocene tephra layers. Bull. Volcanol. 70, 475–493.
Óladóttir, B.A., Larsen, G., Sigmarsson, O., 2011. Holocene volcanic activity at Grímsvötn, Bárðarbunga and Kverkfjöll subglacial centres beneath Vatnajökull, Iceland. Bull. Volcanol. 73, 1187–1208.
Óladóttir, B.A., Sigmarsson, O., Larsen, G., Devidal, J.-L., 2011b. Provenance of basaltic tephra from Vatnajökull subglacial volcanoes, Iceland, as determined by major- and trace-element analyses. Holocene 21, 1037–1048.
Olsen, J., Björck, S., Leng, M.J., Guðmundsdóttir, E.R., Odgaard, B.V., Lutz, C.M., Kendrick, C.P., Andersen, T.J., Seidenkranz, M.-S., 2010. Lacustrine evidence of Holocene environmental change from three Faroese lakes: a multiproxy XRF and stable isotope study. Quat. Sci. Rev. 29, 2764–2780.
Pearce, N.J.G., Westgate, J.A., Preece, S.J., Eastwood, W.J., Perkins, W.T., 2004. Identification of Aniakchak (Alaska) tephra in Greenland ice core challenges the 1645 BC date for Minoan eruption of Santorini. G-cubed 5. https://doi.org/10.1029/2003GC000672.
Pearson, C., Sigl, M., Burke, A., Davies, S., Kurbatov, A., Severi, M., Cole-Dai, J., Innes, H., Albert, P.G., Helmick, M., 2022. Geochemical ice-core constraints on the timing and climatic impact of Aniakchak II (1628 BCE) and Thera (Minoan)

volcanic eruptions. PNAS Nexus 1, 1–12.
Persson, C., 1966. Försök till tefrokronologisk datering av några svenska torvmossar. Geol. Foren. Stockh. Forh. 88, 361–394.
Pilcher, J.R., Hall, V.A., 1992. Towards a tephrochronology for the Holocene of the north of Ireland. Holocene 2, 255–259.
Pilcher, J.R., Hall, V.A., 1996. Tephrochronological studies in northern England. Holocene 6, 100–105.
Pilcher, J.R., Hall, V.A., McCormac, F.G., 1995. Dates of Holocene Icelandic volcanic eruptions from tephra layers in Irish peats. Holocene 5, 103–110.
Pilcher, J.R., Hall, V.A., McCormac, F.G., 1996. An outline tephrochronology for the Holocene of the north of Ireland. J. Quat. Sci. 11, 485–494.
Pilcher, J.R., Bradley, R.S., Francus, P., Anderson, L., 2005. A Holocene tephra record from the lofoten islands, arctic Norway. Boreas 34, 136–156.
Plunkett, G., 2006. Tephra-linked peat humification records from Irish ombrotrophic bogs question nature of solar forcing at 850 cal. yr BC. J. Quat. Sci. 21, 9–16.
Plunkett, G., Pilcher, J.R., 2018. Defining the potential source region of volcanic ash in northwest Europe during the Mid- to Late Holocene. Earth Sci. Rev. 179, 20–37.
Plunkett, G.M., Pilcher, J.R., McCormac, F.G., Hall, V., 2004. New dates for first millennium BC tephra isochrones in Ireland. Holocene 14, 780–786.
Plunkett, G.M., Sigl, M., McConnell, J.R., Pilcher, J.R., Chellman, N.J., 2023. The significance of volcanic ash in Greenland ice cores during the Common Era. Quat. Sci. Rev. 301. https://doi.org/10.1016/j.quascirev.2022.107936.
Ponomareva, V., Polyak, L., Portnyagin, M., 2018. Holocene tephra from the Chukchi-Alaskan margin, Arctic Ocean: implications for sediment chronostratigraphy and volcanic history. Quat. Geochronol. 45, 85–97.
Pyne O'Donnell, S.D.F., Hughes, P.D.M., Froese, D.G., Jensen, B.J.L., Kuehn, S.C., Mallon, G., Amesbury, M.J., Charman, D.J., Daley, T.J., Loader, N.J., Mauquoy, D., Street-Perrot, F.A., Woodman-Ralph, J., 2012. High-precision ultra-distal Holocene tephrochronology in north America. Quat. Sci. Rev. 52, 6–11.
Ratcliffe, J., Andersen, R., Anderson, R., Newton, A., Campbell, D., Mauquoy, D., Payne, R., 2018. Contemporary carbon fluxes do not reflect the long-term carbon balance for an Atlantic blanket bog. Holocene 28, 140–149.
Reimer, P.J., Austin, W.E.N., Bard, E., Bayliss, A., Blackwell, P.G., Bronk Ramsey, C., Butzin, M., Cheng, H., Edwards, R.L., Friedrich, M., Grootes, P.M., Guilderson, T.P., Hajdas, I., Heaton, T.J., Hogg, A.G., Hughen, K.A., Kromer, B., Manning, S.W., Muscheler, R., Palmer, J.G., Pearson, C., van der Plicht, H., Reimer, R.W., Richards, D.A., Scott, E.M., Southon, J.R., Turney, C.S.M., Wacker, L., Adolphi, F., Büntgen, U., Capano, M., Fahrni, S.M., Fogtmann-Schulz, A., Friedrich, R., Köhler, P., Kudsk, S., Miyake, F., Olsen, J., Reinig, F., Sakamoto, M., Sookdeo, A., Talamo, S., 2020. The IntCal20 northern hemisphere radiocarbon age calibration curve (0–55 cal kBP). Radiocarbon 62, 725–757.
Schomacker, A., Brynjólfsson, S., Andreassen, J.M., Gudmundsdóttir, E.R., Olsen, J., Odgaard, B.V., Håkansson, L., Ingólfsson, Ó., Larsen, N.K., 2016. The Drangajökull ice cap, northwest Iceland, persisted into the early-mid Holocene. Quat. Sci. Rev. 148, 68–84.
Sigmarsson, O., Condomines, M., Fourcade, S., 1992. A detailed Th, Sr and O isotope study of Hekla: differentiation processes in an Icelandic volcano. Contrib. Mineral. Petrol. 112, 20–34.
Sigvaldason, G.E., 1974. The petrology of Hekla and origin of silicic rocks in Iceland, eruption of Hekla 1947–1948. Societas Scientarium Islandica 5, 1–44.
Søndergaard, M.K.B., 2005. Lateglacial and Holocene palaeoclimatic fluctuations on the North Icelandic shelf – foraminiferal analysis, sedimentology and tephrochronology of core MD992275. Ph.D. Thesis. University of Aarhus. Aarhus Geoscience 26, 140.
Stivrins, N., Wulf, S., Wastegård, S., Lind, E.M., Alliksaar, T., Galka, M., Andersen, T.J., Heinsalu, A., Seppä, H., Veski, S., 2016. Detection of the Askja AD 1875 cryptotephra in Latvia, eastern Europe. J. Quat. Sci. 31, 437–441.
Sverrisdóttir, G., 2007. Hybrid magma generation preceding Plinian silicic eruptions at Hekla, Iceland: evidence from mineralogy and chemistry of two zoned deposits. Geol. Mag. 144, 643–659.
Swindles, G.T., Outram, Z., Batt, C.M., Hamilton, W.D., Church, M.J., Bond, J.M., Watson, E.J., Cook, G.T., Sim, T.G., Newton, A.J., Dugmore, A.J., 2019. Vikings, peat formation and settlement abandonment: a multi-method chronological approach from Shetland. Quat. Sci. Rev. 210, 211–225.
Thorarinsson, S., 1944. Tefrokronologiska studier på Island. Geogr. Ann. 26, 1–217.
Thorarinsson, S., 1971. The age of the light Hekla layers according to corrected $^{14}C$ datings. Náttúrufræðingurinn 41, 99–105.
Turney, C.S.M., 1998. Extraction of rhyolitic component of Vedde microtephra from minerogenic lake sediments. J. Paleolimnol. 19, 199–206.
Turney, C.S.M., Harkness, D.D., Lowe, J.J., 1997. The use of microtephra horizons to correlate Late-glacial lake sediment successions in Scotland. J. Quat. Sci. 12, 525–531.
Tylmann, W., Bonk, A., Goslar, T., Wulf, S., Grosjean, M., 2016. Calibrating $^{210}Pb$ dating results with varve chronology and independent chronostratigraphic markers: problems and implications. Quat. Geochronol. 32, 1–10.
Vakhrameeva, P., Portnyagin, M., Ponomareva, V., Abbott, P.M., Repkina, T., Novikova, A., Koutsodendris, A., Pross, J., 2020. Identification of Icelandic tephras from the last two millennia in the White Sea region (Vodoprovodnoe peat bog, northwestern Russia). J. Quat. Sci. 35, 493–504.
van den Bogaard, C., Schmincke, H.-U., 2002. Linking the North Atlantic to central Europe: a high-resolution Holocene tephrochronological record from northern Germany. J. Quat. Sci. 17, 3–20.
van der Bilt, W.G.M., Lane, C.S., Bakke, J., 2017. Ultra-distal Kamchatkan ash on Arctic Svalbard: towards hemispheric cryptotephra correlation. Quat. Sci. Rev. 164, 230–235.
Walsh, A.A., Blockley, S.P.E., Milner, A.M., Matthews, I.P., Martin-Puertas, C., 2021. Complexities in European Holocene cryptotephra dispersal revealed in the annually laminated lake records if Diss Mere, East Anglia. Quat. Geochronol. 66, 101213.
Wastegård, S., 2005. Late Quaternary tephrochronology of Sweden: a review. Quat. Int. 130, 49–62.
Wastegård, S., Davies, S.M., 2009. An overview of distal tephrochronology in northern Europe during the last 1000 years. J. Quat. Sci. 24, 500–512.
Wastegård, S., Björck, S., Possnert, G., Wohlfarth, B., 1998. Evidence for the occurrence of Vedde Ash in Sweden: radiocarbon and calendar age estimates. J. Quat. Sci. 13, 271–274.
Wastegård, S., Rundgren, M., Schoning, K., Andersson, S., Björck, S., Borgmark, A., Possnert, G., 2008. Age, geochemistry and distribution of the mid-Holocene Hekla-S/Kebister tephra. Holocene 18, 539–549.
Wastegård, S., Gudmundsdóttir, E.R., Lind, E.M., Timms, R.G.O., Björck, S., Hannon, G.E., Olsen, J., Rundgren, M., 2018. Towards a Holocene tephrochronology for the Faroe Islands, north atlantic. Quat. Sci. Rev. 195, 195–214.
Watson, E.J., Swindles, G.T., Lawson, I.T., Savov, I.P., 2015. Spatial variability of tephra and carbon accumulation in a Holocene peatland. Quat. Sci. Rev. 124, 248–264.
Watson, E.J., Swindles, G.T., Lawson, I.T., Savov, I.P., 2016. Do peatlands or lakes provide the most comprehensive distal tephra records? Quat. Sci. Rev. 139, 110–128.
Watson, E.J., Kołaczek, P., Słowiński, M., Swindles, G.T., Marcisz, K., Gałka, M., 2017a. First discovery of Holocene alaskan and Icelandic tephra in polish peatlands. J. Quat. Sci. 32, 457–462.
Watson, E.J., Swindles, G.T., Lawson, I.T., Savov, I.P., Wastegård, S., 2017b. The presence of Holocene cryptotephra in Wales and southern England. J. Quat. Sci. 32, 439–500.
Wulf, S., Ott, F., Słowiński, M., Noryśkiewicz, A.M., Dräger, N., Martin-Puertas, C., Czymzik, M., Neugebauer, I., Dulski, P., Bourne, A.J., Błaszkiewicz, M., Brauer, A., 2013. Tracing the laacher see tephra in the varved sediment record of the trzechowskies palaeolake in central northern Poland. Quat. Sci. Rev. 76, 129–139.
Wulf, S., Dräger, N., Ott, F., Serb, J., Appelt, O., Guðmundsdóttir, E., van den Bogaard, C., Słowiński, M., Błaszkiewicz, M., Brauer, A., 2016. Holocene tephrostratigraphy of varved sediment records from lakes tiefer see (NE Germany) and czechowskie (N Poland). Quat. Sci. Rev. 132, 1–14.
Zielinski, G.A., Mayewski, P.A., Meeker, D.L., Grönvold, K., Germani, M.S., Whitlow, S., Twickler, M.S., Taylor, K., 1997. Volcanic aerosol records and tephrochronology of the Summit, Greenland, ice cores. J. Geophys. Res. 102, 26625–26640.
Zillén, L.M., Wastegård, S., Snowball, I.F., 2002. Calendar ages of three mid-Holocene tephra layers identified in varved lake sediments in west central Sweden. Quat. Sci. Rev. 21, 1583–1591.